European Cells and Materials Vol.48 2024 (pages 66–92) DOI: 10.22203/eCM.v048a05 ISSN 1473-2262

Original Article

PERIPHERAL BLOOD CELLS ENRICHED BY ADHESION TO CYR61 ARE HETEROGENOUS MYELOID MODULATORS OF TISSUE REGENERATION WITH EARLY ENDOTHELIAL PROGENITOR CHARACTERISTICS

M. Herrmann[1,2,*], J. Schneidereit[2,§], S. Wiesner[2,§], M. Kuric[2], M. Rudert[3], M. Lüdemann[3], M. Srivastava[4], N. Schütze[2], R. Ebert[2], D. Docheva[2] and F. Jakob[2]

[1]IZKF Group Tissue Regeneration in Musculoskeletal Diseases, University Hospital Wuerzburg, 97070 Wuerzburg, Germany
[2]Department of Musculoskeletal Tissue Regeneration, Bernhard-Heine-Center for Locomotion Research & Orthopaedic Hospital Koenig-Ludwig-Haus, University of Wuerzburg, 97074 Wuerzburg, Germany
[3]Department of Orthopedic Surgery, Koenig-Ludwig-Haus, University of Wuerzburg, 97074 Wuerzburg, Germany
[4]Core Unit Systems Medicine, University Hospital Wuerzburg, 97070 Wuerzburg, Germany
[§]These authors contributed equally.

Abstract

Introduction: Circulating precursor cell populations of various lineages have been identified with putative functions in tissue regeneration, which may have potential for cell based individual regenerative strategies. We previously demonstrated the enrichment of an angiogenic precursor cell population from peripheral blood mononuclear cells by CYR61, a protein of the CCN family. *In vivo*, CYR61 mediates the binding of leukocytes and particular monocyte populations at sites of vascular inflammation. **Methods**: We present an *in vitro* enrichment system mimicking (patho) physiology and at the same time representing an effective tool for enrichment of the CYR61-binding blood cells and analyzed this cell population in depth. **Results**: In comparison to fibronectin coating, which is commonly used for selection of endothelial progenitor cells (EPC), CYR61-based enrichment resulted in 8-fold higher cell yields. The CYR61-enriched cell population harbors features of both, early EPC and the monocyte macrophage lineage and therefore represents myeloid angiogenic cells (MAC). This is supported by RNAseq of CYR61-enriched cells and flow cytometry analysis of CD11b expression and acLDL uptake. Functional assays showed that CYR61-enriched MAC have the ability to develop a multinucleated osteoclast-like phenotype as well as to support and participate in angiogenic networks in Matrigel assays. Interestingly, co-cultured CYR61-enriched MAC and their supernatants inhibit mineralization of mesenchymal stromal cells (MSC) during *in vitro* osteogenic differentiation. Further, osteopontin is highly abundant in our CYR61-enriched MAC as confirmed on mRNA and protein level. **Conclusion**: The CYR61-enriched MAC, as an autologous source, may represent both a mirror of certain individual regeneration capacities and an important tool to modulate tissue regeneration.

Keywords: Myeloid angiogenic cells, endothelial progenitor cells, cell therapy, regeneration.

***Address for correspondence**: M. Herrmann, IZKF Group Tissue Regeneration in Musculoskeletal Diseases, University Hospital Wuerzburg, 97070 Wuerzburg, Germany; Department of Musculoskeletal Tissue Regeneration, Bernhard-Heine-Center for Locomotion Research & Orthopaedic Hospital Koenig-Ludwig-Haus, University of Wuerzburg, 97074 Wuerzburg, Germany. Email: marietta.herrmann@uni-wuerzburg.de

Introduction

Circulating precursor cells have been extensively characterized during the last 2–3 decades describing a variety of populations, including endothelial progenitor cell populations with hematopoietic origin, with putative functions in tissue regeneration and possibly interorgan communication. Mature bone marrow provides a lifelong source of circulating precursors with regenerative capacity, which may be useful targets and tools to support *in vitro* and *in situ* tissue engineering and regeneration strategies (Fadini *et al*., 2020a; Girousse *et al*., 2021). In depth characterization of such population may also serve as a diagnostic tool in that they reflect the adaptive response capacity to both physiological and pathological challenges such as exercise or dis-

ease (Fadini *et al*., 2020b; Mohandas *et al*., 2021; Schmid *et al*., 2021; Soltero *et al*., 2021).

Endothelial cells (EC) regulate angiogenesis, support tissue homeostasis and regeneration (Rafii *et al*., 2016) while prespecified EC may even organize tissue macroarchitecture as described for bone and bone marrow (Chen *et al*., 2020; Itkin *et al*., 2016; Kusumbe *et al*., 2014; Rafii *et al*., 2016; Ramasamy *et al*., 2016; Ramasamy *et al*., 2014; Sivaraj and Adams, 2016; Stucker *et al*., 2020). In adult life, EC precursors, endothelial progenitor cells (EPC), are residents in all tissues of the body including bone and its marrow compartments in and around their respective vessel structures (Basile and Yoder, 2014; Rafii *et al*., 2016; Yoder, 2018). However, several mobile populations of EPC can be harvested from the circulation, like the first described CD34+ EPC population (Asahara *et al*., 1997). Since then, a clear definition of true EPC and a characteristic surface marker for these cells are still lacking. One of the heterogeneous subpopulations described was called "early EPC", later also named "circulating angiogenic cells" (CAC) or myeloid angiogenic cells (MAC) (Medina *et al*., 2017; Medina *et al*., 2010; Rehman *et al*., 2003), whose enrichment was enhanced in most cases by fibronectin coating of culture dishes (Rehman *et al*., 2003). Such "early EPC" from the peripheral blood display features of EC but also of a monocyte/macrophage CD14+ phenotype (reviewed in (Varol *et al*., 2015)). These findings initiated discussions about the plasticity of myeloid/monocytic cells to develop towards an EC phenotype (Chopra *et al*., 2018). Their potential of participation in vessel formation is still a matter of debate (Hernandez and Iruela-Arispe, 2020) but it seems evident that their main angiogenic functions are of paracrine nature (Grunewald *et al*., 2006). This is in contrast to more mature EPC populations, also referred to as endothelial colony forming cells (ECFC) or outgrowth endothelial cells (OEC), whose isolation is based on collagen-coating (Mead *et al*., 2008). These cells have been shown to promote vascularization in ischemic diseases and bone defects (Herrmann *et al*., 2014; Herrmann *et al*., 2018; Kawakami *et al*., 2017; Kawamoto *et al*., 2009; Medina *et al*., 2010).

Erythro-myeloid progenitors (EMPs) have been shown to contribute endothelial cells to blood vessels during embryonic development (Plein *et al*., 2018). Likewise, EMPs give rise to monocytic cells, which harbor the potential to differentiate in macrophages and orchestrate tissue homeostasis via regeneration and repair as it was impressively shown for bone remodeling (Yahara *et al*., 2021).

Circulating monocytic cells have a limited half-life (1–7 days) and consist of two main populations namely CD14++CD16+/- "inflammatory" or "classical" monocytes (appr. 90 %) that are highly responsive to inflammatory stimuli, an intermediate population (appr. 10 % of the latter) and CD14+CD16++ "non- classical" or "patrolling" monocytes, which crawl along the lumen of the micro- and macro-vasculature. The process of crawling and the balance between the classical and the patrolling populations are strongly influenced by activation of the Notch signaling pathway, by the adhesion molecules ICAM 1/2 and by the matricellular protein CYR61/CCN1 with the adhering cell population harboring anti-inflammatory properties. CYR61/CCN1 when released by activated platelets controls the recruitment of monocytic cells to the endothelium (Imhof *et al*., 2016), indicating that CYR61-cell enrichment mimics a (patho)physiological process. Monocytes that are activated while patrolling through adhesion infiltrate tissues and can differentiate towards macrophages with high plasticity and the ability to replenish the pool of tissue resident macrophages (Luque-Martin *et al*., 2021; Orozco *et al*., 2021). Of note, in bone, macrophages couple angiogenesis and bone formation by supporting vessel formation (Kohara *et al*., 2022).

The extracellular matrix (ECM) composition and its related matrix-associated growth and differentiation factors have raised special attention in the context of angiogenesis. The "matricellular concept" involves proteins and their families like SPARC, thrombospondin-1 (TSP-1), tenascin-C (TN-C), osteopontin (SPP1), periostin, R-spondins, fibulins and members of the CCN family (CCN1/Cyr61, CCN2, CCN3) (reviewed in (Murphy-Ullrich and Sage, 2014; Perbal, 2018)). The matricellular protein CYR61 is critically involved in embryonic development of the vascular system and CYR61-deficiency is embryonically lethal in mice (Mo *et al*., 2002). mCYR61/CCN1 is a multidomain protein and as such displays a series of various interaction with cell surface receptors (Crockett *et al*., 2007; Hoß *et al*., 2017; Leu *et al*., 2004; Leu *et al*., 2003; Schmitz *et al*., 2013; Schütze *et al*., 2007; Su *et al*., 2010). In adult life, CYR61 expression has been shown to be upregulated in context of angiogenesis, inflammation and regeneration, it accumulates in the early fracture callus, is positively correlated with homeostasis and healing success in bone and after muscle trauma (Lienau *et al*., 2006; Zhao *et al*., 2018) and is upregulated by mechanotransduction *in vitro* (Seefried *et al*., 2017). Pro-angiogenic effects of CYR61 are exhibited by promotion of EC adhesion through $\alpha v\beta 3$ integrin binding (Kireeva *et al*., 1998) and CYR61 has been shown to target common angiogenic signaling pathways such as Notch or vascular endothelial growth factor (VEGF) (Chintala *et al*., 2015). Confluent signaling exerted by VEGF educates monocyte-derived cells and supports their angiogenic properties including endothelial patrolling and tissue infiltration (Avraham-Davidi *et al*., 2013; Luque-Martin *et al*., 2021). This ability of CYR61 to promote angiogenesis and tissue regeneration *in vivo*, motivated us to test CYR61 protein coatings as a tool to enrich regenerative cell populations from peripheral blood as published earlier (Hafen *et al*., 2018; McNeill *et al*., 2015). Furthermore, the enriched cell population reflects the population of blood cells bind-

ing to CYR61 at sites of vascular inflammation (Imhof *et al*., 2016; Löbel *et al.*, 2012) and thus enabled us to gain important insights in the characteristics of this cell population.

Using CYR61 coating as a model for monocyte adhesion to endothelia and as a tool for enrichment, we enrich an apparently MAC population. Here, we characterize the signatures and functions of this population in more detail, especially in comparison with published work (Medina *et al*., 2010) showing that these cells besides some "early EPC" characteristics show a monocyte/macrophage like transcriptome, can be differentiated towards the macrophage and osteoclast lineage of differentiation and support the formation of angiogenic networks *in vitro*. Interestingly, our results suggest that these cells *in vitro* inhibit mineralization, the final step of osteogenic differentiation. In conclusion from our data, CYR61-enriched cells are not a classical EPC population but represent myeloid angiogenic cells with a remarkable plasticity.

Materials and Methods

Chemicals have been purchased from Sigma-Aldrich (Merck, Darmstadt, Germany) unless stated otherwise.

Purification of Recombinant CYR61

SF-21 caterpillar (lepidopteran) derived cells were used to express recombinant CYR61-protein (rCYR61) as described previously (Schütze *et al*., 2005). To purify the rCYR61 protein, protein G sepharose columns (1 mL columns) were used connected to a peristatic pump p1 (GE Healthcare, Braunschweig, Germany, Catalog #17-0404-01). Columns were equilibrated with pH 7 buffered phosphate buffered saline (PBS), the cell culture supernatant was applied (volumes between 15–45 mL) at a flow rate of 2 mL per min. Columns were washed with 10 column volumes of PBS and the protein was eluted with elution buffer (0.1 M glycine, pH 2.4). Directly thereafter, eluted fractions were neutralized using 3 M Tris/HCl pH 8. The yield was determined by a conventional Bradford protein assay (Roti®-Quant, Carl Roth, Karlsruhe, Germany, Catalog # K015.1) and silver gel electrophoresis was performed to check purity.

Isolation of Human Peripheral Blood Mononuclear Cells (PBMC) and Bone Marrow Mesenchymal Stromal Cells (MSC)

For PBMC isolation, commercially available buffy coats were obtained from the Blood Donation Service of the Bavarian Red Cross and used within 18–24 h after donation. Only age and gender of the donors, who approved the use of the buffy coats, were disclosed. Buffy coats were diluted 1:4 with 0.9 % NaCl/1 % fetal bovine serum (FBS, Bio&Sell, Feucht, Germany, catalog # BS.FCS 0.500 EUA) solution. Subsequently, 30 mL were layered on 15 mL of Ficoll-Paque™ density gradient solution (Cytiva, Freiburg, Germany, catalog #17144002) in 50 mL centrifugation tubes, respectively and centrifuged at 800 g for 20 min without brake. Mononuclear cells were collected, centrifuged at 300 g for 10 min, washed twice with 30 mL of 0.9 % NaCl/1 % FBS solution and resuspended in 20 mL of EBM-2 medium (Promocell, Heidelberg, Germany, catalog # CC-3156) supplemented with 5 % FBS, 1× penicillin/streptomycin (Capricorn Scientific GmbH, Ebsdorfergrund, Germany) and 50 µg/mL ascorbate-2-phosphate, referred to as MAC propagation medium. PBMC were seeded at a density of 1×10^7 cells/well into rCYR61 coated 6-well plates in 5 mL MAC propagation medium and incubated at 37 °C. CYR61 coating was performed at 5 µg of Fc-tagged CYR61/six well in 1.5 mL PBS over night at room temperature (RT). Controls with fibronectin coating (fibronectin from human plasma, Sigma-Aldrich, catalog # PHE0023) received 10 µg fibronectin/six well in 1 mL PBS over night at 37 °C.

Primary human bone marrow stromal cells (MSC) were isolated from bone marrow from different donors and cultured up to four weeks by a standardized protocol (Müller-Deubert *et al*., 2020). Bone marrow was obtained with informed consent from acetabular reaming of patients undergoing elective hip arthroplasty. The procedure was approved by the local Ethics Committee of the University of Würzburg (permission number 186/18). Briefly, bone marrow preparations were washed with Dulbecco's modified Eagle's medium, (DMEM/F12, Thermo Fisher Scientific, Dreieich, Germany, catalog #31331-028) supplemented with 10 % FBS, 100 U/mL penicillin, 0.1 mg/mL streptomycin, and 50 µg/mL ascorbate-2-phosphate, and centrifuged at 1200 rpm for 5 min. The pellet was reconstituted in medium for 10–20 sec and washed two times, and the supernatants of the washing steps containing the released cells were collected. Cells were centrifuged and seeded at a density of 1.5×10^9 cells per 175 cm^2 culture flask. Adherent cells were washed after 2 days and cultivated until confluence in a humidified atmosphere with 5 % CO_2.

Cell Culture of CYR61-enriched MAC, MSC and Endothelial Cells

For CYR61-enrichment, cells were washed with 0.9 % NaCl/1 % FBS after 2 and 6 days and cultivated in fresh MAC propagation. Subsequently, cells of passage 0, from now on referred to as (CYR61-enriched) MAC, were detached between day 7 and 9 by using 1 mL/well accutase (Capricorn, catalog #ACC-1B) for 30 min at 37 °C and the use of a cell scraper. Cells were centrifuged (5 min at 300 g), resuspended in fresh medium, and seeded at a density of 1×10^6/well into none-coated standard tissue culture plastic six-well plates in 5 mL MAC propagation medium with a medium change every 3–4 days. MAC at passage 0–1 were used for all experiments as indicated.

MSC were provided with fresh propagation medium every 3 days and passaged when reaching 60–80 % confluence. Cells were detached with 1× Trypsin-EDTA (Capricorn, catalog #TYR-1B) for 5 min at 37 °C, centrifuged (5 min at 300 g), resuspended in fresh medium and filtered through a 100 µm filter. Cells were seeded at a density of 1.5×10^4 cells/cm^2 with medium change every 3–4 days. MSC of passage 1–3 were used for all experiments.

Human umbilical vein endothelial cells (HUVEC (Lonza, CC-2519) and HUVEC-GFP (Cellworks, South San Francisco, CA, USA, ZHC-2402)) and human umbilical artery endothelial cells (HUAEC, Promocell, Heidelberg, Germany, C-12202) were cultured in Endothelial cell growth medium 2 (EGM-2, Promocell, C-22111) with full growth factor supplementation.

Endothelial Cell Differentiation of MAC

CYR61-enriched MAC at passage 0 (after culture for 6 days on CYR61-coated plates in MAC propagation medium) were seeded 10^5 cell/well in 4 well chamber slides and cultured 13 days in EGM-2 + supplements (Promocell) with 5 % FCS, 1 % penicillin/streptomycin, 50 µg/mL ascorbate-2-phosphate and 1 ng/mL human VEGF (Promokine, Promocell, A64421).

Macrophage Polarization, Flow Cytometry Analysis and Quantitative PCR (qPCR)

For macrophage polarization experiments, mononuclear cells (MNC) were isolated as described above. 4×10^7 MNC were subsequently seeded in either CYR61-coated or untreated 25 cm^2 culture flasks and cultured for 6 days in DMEM medium (Thermo Fisher Scientific) supplemented with 10 % FCS, 100 U/mL penicillin, 0.1 mg/mL streptomycin and 50 ng/mL M-CSF (recombinant human M-CSF, R&D, 216-MC). Afterwards, cells were incubated for 1 day with 20 ng/mL LPS (lipopolysaccharides from Escherichia coli, Sigma-Aldrich, catalog # L4516) or 20 ng/mL IL-4 (human IL-4 premium grade, Miltenyi Biotech, Bergisch-Gladbach, Germany, catalog #130-093-920) in DMEM for M1 and M2 polarization respectively, or left untreated (M0 control). Cell polarization was assessed by flow cytometry as described below using a combination of the following antibodies (all Thermo Fisher Scientific): CD86-AlexaFluor488 (catalog #53-0869-42), CD80-PerCp-eFluor710 (catalog #53-0869-42), CD206-Pe-Cy7 (catalog #25-2069-42) and CD163-SuperBright 600 (catalog #63-1639-42). These experiments were repeated with cells from 4 different PBMC donors. In addition, cell polarization was confirmed by qPCR (see below) for 2 donors.

Osteoclastic Differentiation of MAC

CYR61-enriched MACs at passage 0 (after culture for 6 days on CYR61-coated plates in MAC propagation medium) were seeded in a 4 well chamber slide and cultivated for 7 days in DMEM high glucose medium (Capricron, catalog #DMEM-HA) with 5 % FCS, 1 % penicillin/streptomycin, 50 µg/mL ascorbate-2-phosphate, 25 ng/mL macrophage colony-stimulating factor (M-CSF, R&D Systems, Minneapolis, MN, catalog #216-MC-010) and 50 ng/mL receptor Activator of NF-κB Ligand (RANKL, R&D, catalog #6449-Tec).

Osteogenic Differentiation of MSC

To test the influence of MAC on osteogenic differentiation of MSC, a standard *in vitro* osteogenic differentiation protocol for MSC was applied with the addition of MAC (direct co-culture) or MAC conditioned medium (MAC-CM) either for the entire differentiation period of 28 days or the after 2 weeks of pre-differentiation of MSC. For this, $1.5–2.0 \times 10^6$ MSCs were seeded on a six well plate and cultured in propagation medium until 100 % confluence. Then cells were cultured in osteogenic differentiation medium (DMEM high glucose supplemented with 10 % FCS, 100 U/mL penicillin, 0.1 mg/mL streptomycin, 50 µg/mL ascorbate-2-phosphate, 10 mM beta-glycerophosphate and 100 nM dexamethasone). For direct co-cultures, after 14 days either 1.5×10^6 cells of MACs were added to a six well and cultured for another 14 days in mixture medium of 50 % DMEM high Glucose Medium and 50 % EGM medium supplemented with 50 µg/mL ascorbate-2-phosphate, 10 mM beta-glycerophosphate and 100 nM dexamethasone. To test the effect of MAC-CM, MSC were cultured for the full differentiation period or after 14 days with a mixture of 50 % MAC-CM (collected from p0 MAC cultures in MAC propagation medium between d6 and d9) and 50 % DMEM high glucose medium with 50 µg/mL ascorbate, 10 mM beta-glycerophosphate and 100 nM dexamathasone.

Mineral deposition after 28 days was assessed by Alizarin Red S staining. For this, cells were washed once with PBS and fixed with ice cold methanol for 10 min at RT. After one washing step, they were stained with a 1 % Alizarin Red S staining solution pH 4.4 for 2 min at RT. After 3 more washing steps, cells were fixed and plates dried.

For semi-quantitative evaluation of mineralization, images were taken light microscopally (Axio Observer 7, Zeiss, Jena, Germany) and the percentage of stained area calculated in ImageJ (version 1.52, Rasband, NIH, Bethesda, MD, USA).

Staining of Cells with Cell Tracker

Cell Tracker® Orange CMTMR (5-(and-6)-(((4-chloromethyl)benzoyl)amino)tetramethyl-rhodamine, Thermo Fisher Scientific, catalog #C34551) was used according to the manufacturer‘s instructions. Briefly, MAC at 80–90 % confluence were stained in six well plates in serum-free medium with 1.5 mL of a 2 µM reagent solution, incubated at 37 °C for 45 min, washed with fresh medium and incubated in propagation medium.

Immuncytochemistry

HUAC p6, HUVEC p6, MSC p0, MAC p0 were seeded at a density of 10^5 cells per well in 4-well chamber slides for 7 days in propagation medium.

Phalloidin Staining

Cells were rinsed with PBS and fixed with 4 % paraformaldehyde. Phalloidin (Biotum inc. Fremont, CA, USA, catalog #Cf488A) staining was performed according to the manufacturer's protocol. Cells were mounted in mounting medium with DAPI (Vector Laboratories, Newark, CA, USA, catalog #H1200). Staining was visualized using a Zeiss Axiovert A1 with ZEN Software (Zeiss).

Vimentin Staining

Formalin fixed cells were washed 5 min in PBS. Quenching of endogenous peroxidase was performed with 3 % H_2O_2 for 10 min. After washing with PBS, diluted blocking serum (Vectastain Elite ABC Kit, Peroxidase (Goat IgG), Merck, catalog # K29043897) was added and incubated for 20 min. Excess serum was tipped off and slides incubated for 1 hour with primary anti-vimentin antibody (R&D, catalog #AF 2105, at 0.25 µg/µL diluted 1:100 in PBS with 2.5 % serum). Cells were washed for 5 min in PBS, incubated for 30 min with biotinylated secondary antibody 1:200, washed for 5 min in PBS and were finally incubated for 30 min with Vectastain Elite ABC Reagent. Cells were then washed for 5 minutes in PBS, incubated for 10 min in peroxidase substrate kit (Vector Nova Red, Vector Laboratories, catalog #SK-4800). Finally, cells were rinsed in tap water and counterstained with Hemalaun Mayer and visualized as described above.

Tartrate Resistant Acid Phosphatase (TRAP) Staining

The acid phosphatase staining was carried out using procedure 387 from Sigma-Aldrich on MACs after culture under endothelial or osteoclastic differentiation conditions. Cells were rinsed in PBS, fixed and stained according to the manufacturer's protocol. Imaging was performed as described above.

Gene Expression Analysis

RNA Isolation and cDNA Synthesis

At indicated time points cells were harvested and RNA was isolated using the GF-1 total RNA extraction kit (GeneOn Bio Science, Ludwigshafen, Germany, catalog #GF-1TR100) according to the manufacturer's instructions. RNA concentration was determined and 1 µg of RNA reversed transcribed by using MMLV Reverse Transcriptase (Promega, Walldorf, Germany, catalog # M1708) according the manufacturer's protocol using random hexamer primers (Promega). The resulting cDNA was used immediately or stored at – 20 °C.

Semi-quantitative RT-PCR

RT-PCR was performed with GO Taq G2 Flexi Polymerase (Promega, catalog # M7806) in a total volume of 30 µL containing 6 µL 5× Promega reaction buffer, 1 µL 10 mM dNTP (Bioline, Meridian Bioscience, Luckenwalde, Germany), 3 µL 25 mM $MgCl_2$, 1 µL 5 pmol/µL specific forward and reverse primer (Table 1), 1 µL cDNA and 0.2 µL 5 U/µL GO Taq G2 Flexi polymerase. PCR amplification was performed as follows: initial denaturation at 94 °C for 5 min; 23–40 cycles of denaturation at 94 °C for 30 sec; annealing temperature (Table 1) for 30 sec; elongation at 72 °C for 45 sec, and a final amplification step at 72 °C for 5 min in a Peqstar cycler (Peqlab, VWR, Darmstadt, Germany). PCR products were visualized under UV light by gel electrophoresis on a 1.5 % agarose gel containing GelRed® (Genaxxon Bioscience GmbH, Ulm, Germany, catalog #S445L).

Quantitative PCR (qPCR)

For selected target genes, qPCR analysis was performed by using the GoTaq® qPCR system (Promega, catalog #A6002) and 0.25 pmol/µL sequence-specific primers (Eurofins Genomics GmbH, Ebersberg, Germany) in a qTower (Analytic Jena, Jena, Germany). Primer sequences and PCR conditions are listed in Table 2. After an initial denaturation step at 94 °C for 3 min, amplification was generally repeated 40 times (denaturation: 10 sec 94 °C; annealing 10 sec 57–61 °C; elongation 20 sec 72 °C), every cycle being followed by a plate read. Melting curve analysis (65 °C to 95 °C, increments of 0.5 °C for 5 sec) was performed for amplicon specificity analysis Relative target gene expression was calculated using the ΔΔCt method (Pfaffl, 2001). Values were normalized to the reference gene expression of ribosomal protein, large, P0 (RPLP0).

Flow Cytometry Analysis

Surface marker staining and uptake of acetylated low density lipoprotein (acLDL) was assessed in MAC after 7 and 14 days of endothelial differentiation or after 14 days of exposure to osteoclast differentiation medium as described above. PBMCs incubated in standard osteoclast differentiation medium (see above) served as control. Cells were detached and cell count determined. To investigate acLDL uptake, 0.5–1 × 10^6 cells were washed with buffer (PBS/1 % FBS) and exposed to 10 µg/mL acLDL (low density lipoprotein from human plasma acetylated dil complex (Thermo Fisher Scientific, catalog # L23380)) for 4 h at 37 °C. After a washing step to remove remaining acLDL in the supernatant, cells were exposed to anti-human Fc Receptor Binding Inhibitor at 1 mg/mL (Thermo Fisher Scientific, Catalog # 14-9161-73) for 20 min on ice to reduce unspecific antibody binding. Afterwards, cells were stained with the following antibodies (all Thermo Fisher Scientific) according the manufacturer's recommendations: CD11b-APC-eF780 (Catalog # 47-0112-82), CD14-eF450 (Cata-

Table 1. Primer sequences and conditions of RT-PCR.

Gene	Tm	Size	NM number	Sequence forward	Sequence reverse
EEF1α	54 °C	369 bp	NM_001402.6	CTGTATTGGATTGCCACACG	AGACCGTTCTTCCACCACTG
OCT4	55 °C	360 bp	NM_001173531.2	CCGCCGTATGAGTTCTGTG	GATGGTCGTTTGGCTGAATA
SOX2	55 °C	260 bp	NM_003106.4	CCCCTGTGGTTACCTCTTCC	CCTCCCATTTCCCTCGTTTT
NANOG	55 °C	500 bp	NM_001297698.2	TTCCTTCCTCCATGGATCTG	ATTGTTCCAGGTCTGGTTGC
CXCR 4	55 °C	269 bp	NM_001008540.2	CATCCTGGTCATGGGTTACC	TCCTTGGCCTCTGACTGTTG
CXCL12	55 °C	160 bp	NM_199168.4	TCAGCCTGAGCTACAGATGC	CTTTAGCTTCGGGTCAATGC
PECAM1	55 °C	300 bp	NM_000442.5	TCCGATGATAACCACTGCAA	GTGGTGGAGTCTGGAGAGGA
CD14	56 °C	176 bp	NM_000591.4	GGAAGACTTATCGACCATGGAGC	GGAAGACTTATCGACCATGGAGC
CD34	55 °C	400 bp	NM_001025109.2	CTTTCTCCTGTGGGGCTCCA	TGACTCAGGGCATCTGCCTG
EMCN	57 °C	516 bp	NM_001159694.1	GAGTCTGGTGAGCACTCTGC	CGTGCAACTTTTCCCTGCAT
VWF	55 °C	213 bp	NM_000552.4	CATTGGTGAGGATGGAGTCC	AGCACTGGTCTGCATTCTGG
VCAM	53 °C	265 bp	NM_001078.4	TTTCTGGAGGATGCAGACAG	GTAGACCCTCGCTGGAACAG
ANGPTL4	56 °C	207 bp	NM_139314.3	GCCTATAGCCTGCAGCTCAC	GGATGGAGCGGAAGTACTGG
KDR	56 °C	150 bp	NM_002253.3	GACTTTGAGCATGGAAGAGGA	CGGCTCTTTCGCTTACTGTT
FLT1	51 °C	168 bp	NM_001159920.2	GGCACAGAGACCCAAAAGAA	AGTCCTCAGAGAAGGCAGGA
FLT4	55 °C	277 bp	NM_001354989.1	TGGTGCACATCACAGGCAAC	TTGGCCTTGCACACATACGA
TIE1	51 °C	164 bp	NM_005424.5	CACCGCTGTACTTTCTGCAT	CACTGTAGATGCCGCTCGAT
TIE2	48 °C	154 bp	NM_000459.5	GCCTTCACCAGGCTGATAGT	TCTCACACGTCCTTCCCATA
SPP 1 Iso A		288 bp	NM_001040058.2		
Iso B	55 °C	246 bp	NM_000582.3	ATGAGAATTGCAGTGATTTGCTTTTGCCT	CATGGTCATCATCATCTTCATCATC
Iso C		207 bp	NM_001040060.2		
COL1A1	54 °C	152 bp	NM_000088.4	ATGGCATCCCTGGACAGC	AGACCACGAGGACCAGAGG
ALPL	51 °C	454 bp	NM_000478.6	TGGAGCTTCAGAAGCTCAACACCA	ATCTCGTTGTCTGAGTACCAGTCC
IL1bβ	58 °C	368 bp	NM_000576.3	GAAGTACCTGAGCTCGCCATGGAA	CGTGCAGTTCAGTGATCGTACAGG
VEGFα	55 °C	165 bp	NM_003376.6	TCTTCAAGCCATCCTGTGTG	TGTTGTGCTGTAGGAAGCTCA
TNF	55 °C	123 bp	NM_000594.4	GCCCCAATCCCTTTATTACC	TCGAAGTGGTGGTCTTGTTG
CSF1	55 °C	421 bp	NM_172212.3	CGTCCGAACTTTCTATGA	CGATGGTGCTGTCCTT
FSTl3	55 °C	198 bp	NM_005860.3	ACCTGAGCGTCATGTACCG	TGTGGCACGAGGAGATGTAG

log # 48-0149-42), CD31-PeCy7 (Catalog # 25-0311-82), CD45-eF506 (Catalog # 69-0459-42), CD146-PE (Catalog # 12-1469-42). Measurements were performed using an Attune NxT Flow Cytometer (Thermo Fisher Scientific) and data were analyzed in FlowJo v10, Ashland, OR, USA.

RNA Sequencing and Data Analysis

RNA extracted from MAC (used at p0–p1, culture in MAC propagation medium) and HUVEC (p5–p8) was used for RNA sequencing. DNA libraries suitable for sequencing were prepared from 500 ng of total RNA from all samples with oligo-dT capture beads for poly-A-mRNA enrichment using the TruSeq Stranded mRNA Library Preparation Kit (Illumina, Berlin, Germany). Sequencing was performed on the NextSeq-500 platform (Illumina) in single-end mode with 1 × 75 nt read length with 21–28 million reads/sample. Sequencing data are available at available at European Genome-Phenome Archive (https://ega-archive.org/) (Freeberg *et al*., 2022). Illumina reads were quality- and adapter-trimmed using Cutadapt version 2.5 with a cut-off Phred score of 20 in NextSeq mode, discarding reads without any remaining bases (command line parameters: –nextseq-trim = 20 -m 1 -a AGATCGGAAGAGCACAC-GTCTGAACTCCAGTCAC). The quality filtered reads were mapped against the human reference genome (GCF_000001405.39_GRCh38.p13) using STAR v2.7.2b (Dobin *et al*., 2013) with de-fault parameters. FeatureCounts v1.6.4 (Liao *et al*., 2014) was used for assigning sequence reads to genomic features. The BioConductor package DESeq2 1.24.0 (Love *et al*., 2014) was used to identify genes that were significantly differentially expressed between the different conditions, following standard normalization procedures. Genes with log2 fold change ≥ 1 and $padj < 0.05$ were considered significantly differentially expressed. Pathway analysis was con-ducted using the GSEA function of clusterProfiler (Yu *et al*., 2012) version 3.12.0 for gene set enrichment analysis based on the Kyoto Encyclopedia of Genes and Genomes (KEGG) path-ways.

The expression of markers genes in RNA sequencing data was compared to the available expression data (GSE20283) for EPC subtypes and monocytes to curate and validate the identified markers. Spearmann corelation was calculated by comparing log transformed microarray data with our RNAseq dataset. The row Z-score plots presented

Table 2. Primer sequences and conditions of qPCR.

Gene	Tm	Size	NM number	Sequence forward	Sequence forward	Efficiency
Osteogenic differentiation						
RPLPO	60	125	NM_001002.4	tgcatcagtaccccattctatcat	aggcagatggatcagccaaga	2.01
RUNX2	58	147	NM_001024630.4	cttcacaaatcctccccaag	atgcgccctaaatcactgag	1.91
ALPL	58	151	NM_000478.6	gtacgagctgaacaggaacaacg	cttggcttttccttcatggtg	1.83
IBSP	57		NM_004967.4	Primer Hs_IBSP_1_SG (Qiagen)		1.85
Macrophage polarization						
GAPDH	58		NM_002046.7	Hs_GAPDH_1_SG (Qiagen)		1.96
ACTB	58		NM_001101.5	Hs_ACTB_1_SG		2.08
IL 1b	60	120	NM_000576.3	gacctgagcaccttctttccc	gcacataagcctcgttatccc	1.82
IL 6	60	153	NM_000600.5	ggcatctcagccctgagaaag	caccaggcaagtctcctcatt	1.85
CD 163	60	85	NM_004244.6	gtgcctgttttgtcaccagttc	ttacacaccgttccccactcc	1.83
MRC1	60	156	NM_002438.4	tccaaacgccttcatttgcc	gcttttcgtgcctcttgcc	1.88

in Fig. 2 provide hints of the comparable expression for both the RNA sequencing data as well as GSE20283 data.

Matrigel Tube Formation Assays

To assess the angiogenic potential of MAC, a 2D tube formation on Matrigel was performed. A well of a 48 well plate was coated with 150 µL growth factor containing Matrigel (Corning, New York, USA, catalog #CLS354262). Matrigel-coated wells were seeded with GFP-HUVEC (p5–p7) or cell tracker labeled MAC (p0) at a density of 6×10^4 cells per well in monoculture or co-culture of 10 % MAC and 90 % HUVEC and cultured in 150 µL EGM-2 medium (Promocell). Pictures were acquired during the first 24 h of culture using a fluorescence microscope (DMi8, Leica Microsystems, Wetzlar, Germany).

OPN Detection by Western Blotting and ELISA

MAC were incubated 24 h with propagation medium without FBS. The supernatant was collected and concentrated with Amicon Ultra centrifugal filters 30K (Merck, catalog #2408) according to the manufacturer's protocol. For western blot, 30 µg protein (protein concentration was measured as described in 2.1) was added to the appropriate amount of 6× Laemmlibuffer and heated to 95 °C for 5 min. Proteins were separated by SDS PAGE with a 10 % polyacrylamide gel using 150 V and blotted by semidry blotting method onto a PVDF membrane for 2 h with 150 mA per membrane. The membrane was blocked for 2 h at RT in 5 % solution of skimmed milk in TBS-T (0.1 %). The primary antibody against OPN (R&D, AF 1433) was incubated over night at 4 °C in a concentration of 1 µg/mL in blocking solution. After washing the membrane 3 times for 20 min at RT in TBS-T (0.1 %), it was incubated with an anti-goat HRP-conjugated secondary antibody in blocking solution 1:1000 for 1 h at RT. Three washing steps with TBS-T at RT for 20 min followed, before signals were detected using the WesternBright Sirius Western blotting detection kit (Advansta, San Jose, CA, USA, catalog # K-12043-D20) according to the manufacturer's protocol.

For quantification of OPN in cell culture supernatants, a human osteopontin immunoassay (R&D, Quantikine, DOST00) was used according to the manufacturer's protocol.

Statistics

All values are given as mean ± standard deviation. Statistical analyses were performed using GraphPad Prism software (v10, La Jolla, CA, USA). Normal distribution of data was confirmed by the Shapiro-Wilk test and subsequently an unpaired *t*-test, Mann-Whitney, Kruskal-Wallis or Two-way ANOVA with Tukey's Multiple Comparison test applied dependent on the number of experimental groups and variables. Wilcoxon Signed Rank Test was used for normalized qPCR results. A p-value < 0.05 was considered as statistically significant.

Results

CYR61-enriched MAC Harbor Features of Both Early EPC and the Monocyte/Macrophage Lineage

Our earlier work (Hafen *et al*., 2018) demonstrated that enrichment of peripheral blood mononuclear cells on CYR61 results in an adherent cell population that acquires features of early EPC upon culture in endothelial medium. Moreover, *in vivo* CYR61 has been shown to attract leukocytes and monocyte populations in the circulation (Imhof *et al*., 2016; Löbel *et al*., 2012). We here aimed to further analyze this cell population and to determine possible regenerative functions. In comparison to fibronectin coating, commonly used for selection of EPC populations, an in average 8.5-fold higher cell yield could be obtained upon CYR61-enrichment (Fig. 1**A**). Phase contrast microscopy demonstrated a heterogeneous morphology of the MAC population, containing mostly cells with rounded shape. There was only weak expression of the mesenchymal marker vimentin in comparison with HUAC and HUVEC and MSC (Fig. 1**B**). RT-PCR of selected marker genes (Fig. 1**C**) in such populations reveals stem cell marker expression (e.g., *OCT4*, *SOX2*, *NANOG*) as well as markers of the stem cell

Table 3. Abundance of CD11b-LDL+ and CD11b+LDL+ cells in Cyr61 and Fn-enriched cells.

Cell population	Cyr61	FN	Cyr61	FN
	Day 7		Day 14	
Total CD11b-LDL+	8.49 ± 3.85	9.10 ± 5.47	5.99 ± 3.09*	14.89 ± 2.80
FSC/SSC^{low} CD11b-LDL+	3.64 ± 2.51	3.36 ± 1.02	1.95 ± 0.69	2.48 ± 0.81
FSC/SSC^{high} CD11b-LDL+	4.85 ± 4.39	5.74 ± 4.66	4.04 ± 2.45*	12.41 ± 3.20
Total CD11b+LDL+	19.04 ± 14.30	18.72 ± 13.09	30.80 ± 8.82	14.98 ± 5.07
FSC/SSC^{low} CD11b+LDL+	1.26 ± 1.36	0.48 ± 0 .65	0.83 ± 0.10**	0.18 ± 0.04
FSC/SSC^{high} CD11b+LDL+	17.78 ± 12.93	18.24 ± 12.45	29.97 ± 8.63	14.80 ± 5.03

Statistics: normal distribution confirmed by Shapiro-Wilk Test, significance assessed by unpaired *t*-test, * $p < 0.05$; ** $p < 0.01$. FN, fibronectin.

niche, e.g., *CXCR4* and *CXCL12*, and extracellular matrix *COL1A1*. Otherwise we detected mainly endothelial cell and angiogenesis related (e.g., *CD31*, *VCAM* , *TIE1* ,*KDR* , *FLT1* but also monocyte/macrophage related (e.g., *CD14*, *SPP1* gene expression patterns. Of note, MAC were negative for mature endothelial marker such as *CD34*, *EMCN* and *TIE2* and showed only weak expression of *ANGPTL4* and *VWF* (Fig. 1**C**). Note that in these experiments PCR conditions were adapted to investigate the general presence of the respective transcripts in the different cell population but not quantitative differences between cell populations, which has been the focus of the following RNAseq analysis. Flow cytometry analysis revealed a subpopulation of small cells with low complexity (FSC/SSC^{low}) and big cells with high complexity (FSC/SSC^{high}) that could be reasonably separated based on forward (FSC) and side scatter signals (SSC) (Fig. 1**D**). These populations were detectable after 7 and 14 days of culture on CYR61-coated plates with a shift towards a higher accumulation of big cells at later time points (30.6 ± 12.8 % big cells at day 7 vs. 43.1 ± 13.1 % at day 14). We analyzed expression of CD11b and uptake of acLDL and found that a putative CD11b-LDL+ EC-like population was predominantly abundant in the small population, while big cells contained a high percentage of CD11b+LDL+ monocytes/macrophages. At day 7, no significant changes were detected in comparison to cells enriched on fibronectin (FN). At day 14, significant more CD11b-LDL+ cells were detected in the FN group ($p < 0.05$), while Cyr61-enrichment seemed to favor the CD11b+LDL+ population (Table 3). In addition, CD14 and CD31 positive cells were highly abundant in MAC in a donor dependent manner (data not shown), further confirming the presence of monocytes/macrophages that typically stain positive for these markers.

As a hallmark of the CYR61-enriched endothelial/macrophage (earlyEPC/MAC) population, we found high gene expression of *SPP1*/osteopontin, while EC lines are *SPP1* negative (Fig. 1**C**), which also applies for monocytes from the literature (Medina *et al*., 2010). Western Blot confirmed osteopontin expression and secretion (Fig. 1**E**). Both, RT-PCR and western blot, reveal that the main amplicon and expressed protein represents SPP1 isoform a. This isoform together with isoform c has been described to be very active in neoangiogenesis and limb perfusion in genetically engineered mouse populations (Lee *et al*., 2019; Lok and Lyle, 2019). When we measured protein levels in cell culture supernatants, we found excessively high SPP1/OPN production, up to 1458 ± 273 ng/mL at day 13 of culture (Fig. 1**F**), when compared with MSC secretion as an example of a skeletal precursor cell, where we measured an average of just 1 ng/mL (data not shown).

We then analyzed the transciptomes of our MAC and commercially available HUVEC and compared these results with microarray data from early EPC (eEPC), late outgrowth endothelial cells (OEC) and monocytes reported by Medina *et al*. (2010). When MAC and HUVEC transcriptomes were compared by RNA-Seq 5189 genes were upregulated while 3972 genes were downregulated at *p*adj < 0.05 and log2FC ≥1. The 100 most differentially regulated genes are listed in Tables 4,5. RT-PCR results were taken as a technical evaluation of the RNA-Seq procedure and mirrored the expression data of RNA-Seq (Fig. 2**C**). Similar to the expression pattern suggested by RNA-Seq, VEGFA was equally expressed in both HUVEC and MAC, while *KDR*, *CD34* and *FSTL3* were predominantly expressed in HUVEC. In contrast, *IL1B*, *TNF* and *CSF1* were exclusively expressed or upregulated in MAC, respectively. RNA-Seq data provided evidence for the monocytic/macrophage nature of the CYR61-enriched population. Principle component analyses demonstrated a clear separation of our cell preparation and HUVEC (Fig. 2**A**). Among the differentially expressed genes, several genes of the monocyte/macrophage lineage, including *CD163*, *FCGR3A* (alias CD16) and *MARCO* as well as *SPP1* and *MMP-9*, were significantly upregulated in MAC (Fig. 2**B** and Table 4). String analysis of the 250 genes of highest differential expression (all > log 2-fold) in MAC illustrates gene networks related to the innate immune system, cell adhesion and osteoclast differentiation (Fig. 2**D**), while in HUVEC angiogenesis and circulatory system development pattern were most prominent (Fig. 2**E**).

Gene set enrichment analysis for KEGG pathways (Table 6) resulted among others in significant enrichment of genes related to antigen processing and presenta-

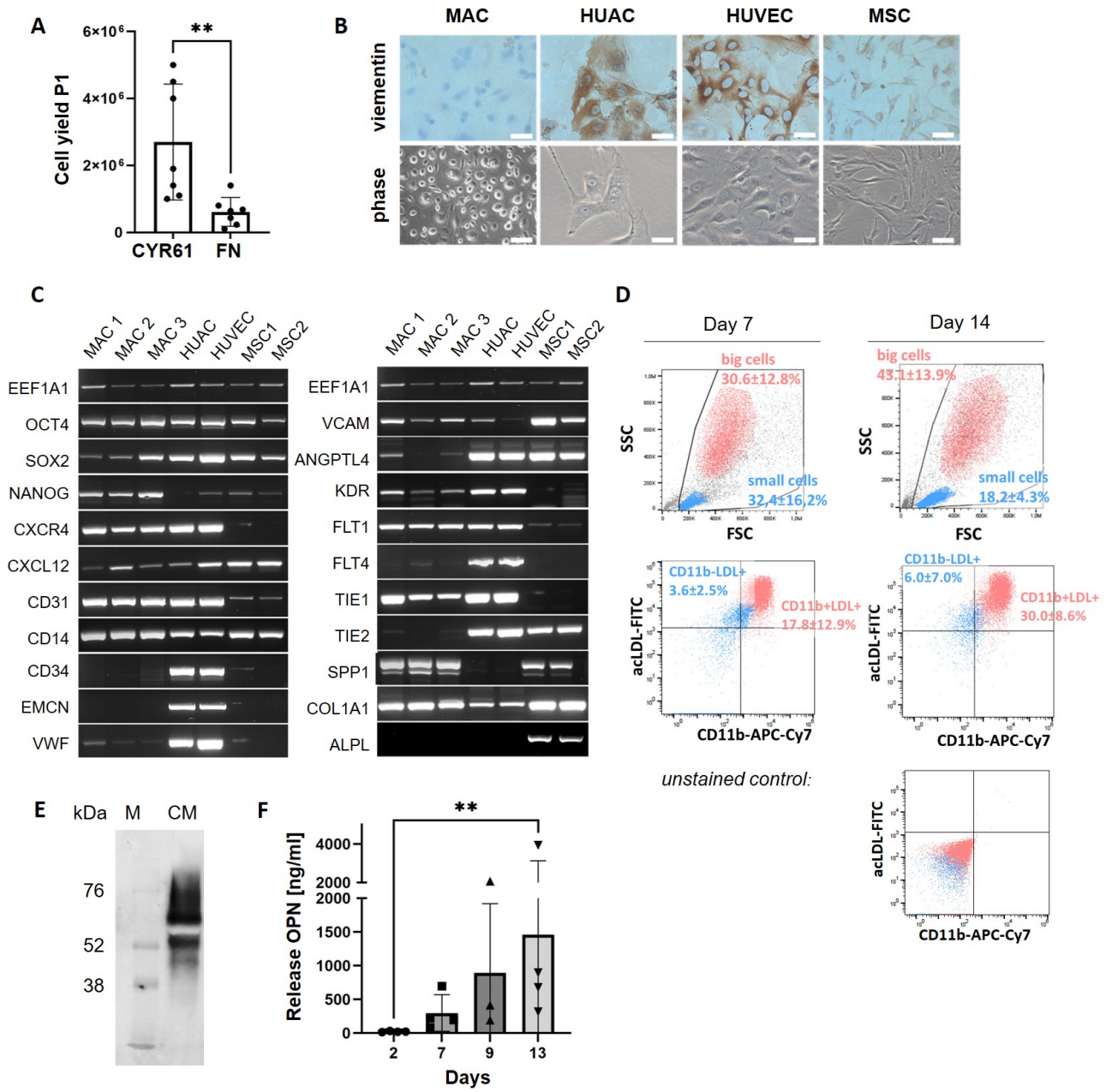

Fig. 1. Characterization of CYR61-enriched MAC in comparison to mature endothelial cell lines and primary bone marrow derived MSC. (**A**) Cell yield in passage 1 (P1) after 14 days of culture on CYR61 or fibronectin (FN) coated plates, respectively; initial seeding density was $1 \times 10^6/cm^2$ Peripheral Blood Mononuclear Cells (PBMC). An unpaired *t*-test was applied to test for statistical significance. ** $p < 0.01$. (**B**) Morphology in phase contrast and vimentin staining. Scale bars = 100 µm. (**C**) RT-PCR based amplification of marker genes; three individual MAC donors are shown and compared with the commercially available arterial and venous endothelial cell lines HUAC and HUVEC and two different donors of bone marrow derived MSC. *EEF1A1* is included as housekeeping gene. (**D**) Flow cytometry analysis of characteristic surface markers and acetylated low density lipoprotein (acLDL) particle uptake. FSC-SSC plots show two distinct cell populations: a small cell population with low complexity (blue) and a big cell population with high SSC signal (red). Quadrant plots on the right indicate that small cells are predominantly CD11b negative and contain a population which is able to take up acLDL (CD11b-LDL+, blue), while big cells are mostly CD11b+LDL+ double positive (red). Gates were set using an unstained control, depicted at the bottom. Percentages present mean ± standard deviation of the entire cell population (day 7: n = 6; day 14: n = 4). (**E**) Western Blot analysis of OPN secreted by MAC measured in MAC-conditioned media (CM), confirming the presence of at least two variants. M, molecular weight marker. (**F**) Quantification of OPN in MAC-CM by ELISA. Kruskal-Wallis test was applied to test for statistical significance. ** $p < 0.01$.

Table 4. Top 100 most differentially upregulated genes.

Gene	Name	Gene ID	log2FC	padj
SLAMF7	SLAM family member 7	57823	14.70	1.87×10^{-35}
HLA-DQA1	major histocompatibility complex2C class II2C DQ alpha 1	3117	14.57	3.66×10^{-74}
CCL3	C-C motif chemokine ligand 3	6348	14.49	4.40×10^{-42}
S100A9	S100 calcium binding protein A9	6280	14.34	4.85×10^{-46}
LAIR1	leukocyte associated immunoglobulin like receptor 1	3903	14.27	1.88×10^{-42}
ADAMDEC1	ADAM like decysin 1	27299	14.12	3.75×10^{-110}
LILRB4	leukocyte immunoglobulin like receptor B4	11006	14.09	8.10×10^{-110}
CHIT1	chitinase 1	1118	14.09	6.25×10^{-66}
CD163	CD163 molecule	9332	14.06	2.44×10^{-74}
HLA-DQA2	major histocompatibility complex2C class II2C DQ alpha 2	3118	14.04	2.08×10^{-30}
CCR1	C-C motif chemokine receptor 1	1230	14.00	5.34×10^{-54}
CYBB	cytochrome b-245 beta chain	1536	13.97	1.27×10^{-152}
C1QA	complement C1q A chain	712	13.94	3.23×10^{-62}
LYZ	lysozyme	4069	13.90	0.00
CD4	CD4 molecule	920	13.88	3.91×10^{-77}
MMP9	matrix metallopeptidase 9	4318	13.87	4.59×10^{-99}
VSIG4	V-set and immunoglobulin domain containing 4	11326	13.85	3.21×10^{-53}
FCGR3A	Fc fragment of IgG receptor IIIa	2214	13.84	2.38×10^{-36}
PLA2G7	phospholipase A2 group VII	7941	13.83	1.46×10^{-87}
TYROBP	TYRO protein tyrosine kinase binding protein	7305	13.82	3.41×10^{-116}
C1QC	complement C1q C chain	714	13.77	1.33×10^{-40}
HLA-DRA	major histocompatibility complex2C class II2C DR alpha	3122	13.76	2.84×10^{-202}
HLA-DRB5	major histocompatibility complex2C class II2C DR beta 5	3127	13.75	8.44×10^{-55}
TMEM176A	transmembrane protein 176A	55365	13.74	1.64×10^{-33}
SPP1	secreted phosphoprotein 1	6696	13.73	3.80×10^{-111}
SLAMF8	SLAM family member 8	56833	13.68	7.69×10^{-54}
CHI3L1	chitinase 3 like 1	1116	13.63	6.60×10^{-54}
GAS7	growth arrest specific 7	8522	13.62	2.42×10^{-39}
DCSTAMP	dendrocyte expressed seven transmembrane protein	81501	13.60	1.22×10^{-34}
CD84	CD84 molecule	8832	13.59	1.69×10^{-129}
MNDA	myeloid cell nuclear differentiation antigen	4332	13.58	7.01×10^{-39}
BIN2	bridging integrator 2	51411	13.58	1.69×10^{-41}
SDS	serine dehydratase	10993	13.56	2.05×10^{-37}
NCF2	neutrophil cytosolic factor 2	4688	13.56	1.42×10^{-60}
FCN1	ficolin 1	2219	13.55	1.06×10^{-40}
FCGR2B	Fc fragment of IgG receptor IIb	2213	13.54	8.47×10^{-32}
HCK	HCK proto-oncogene2C Src family tyrosine kinase	3055	13.53	1.84×10^{-41}
HLA-DRB1	major histocompatibility complex2C class II2C DR beta 1	3123	13.53	5.60×10^{-171}
HLA-DRB6	major histocompatibility complex2C class II2C DR beta 6 28pseudogene29	3128	13.52	1.70×10^{-35}
LILRB5	leukocyte immunoglobulin like receptor B5	10990	13.47	1.14×10^{-19}
SASH3	SAM and SH3 domain containing 3	54440	13.42	1.04×10^{-39}
MARCHF1	membrane associated ring-CH-type finger 1	55016	13.41	1.53×10^{-35}
CSF3R	colony stimulating factor 3 receptor	1441	13.39	7.13×10^{-36}
CSF1R	colony stimulating factor 1 receptor	1436	13.38	2.49×10^{-60}
SLA	Src like adaptor	6503	13.34	3.68×10^{-38}
HLA-DOA	major histocompatibility complex2C class II2C DO alpha	3111	13.33	4.29×10^{-30}
VAV1	vav guanine nucleotide exchange factor 1	7409	13.31	2.35×10^{-37}
ATP6V0D2	ATPase H2B transporting V0 subunit d2	245972	13.30	2.40×10^{-32}
CD52	CD52 molecule	1043	13.30	3.84×10^{-39}
CD53	CD53 molecule	963	13.29	8.39×10^{-121}
MARCO	macrophage receptor with collagenous structure	8685	13.27	2.14×10^{-36}
SLC2A5	solute carrier family 2 member 5	6518	13.25	1.38×10^{-31}
APOC4-APOC2	APOC4-APOC2 readthrough 28NMD candidate29	100533990	13.23	5.35×10^{-33}

Table 4. Continued.

Gene	Name	Gene ID	log2FC	padj
APOC2	apolipoprotein C2	344	13.21	6.99×10^{-33}
FPR3	formyl peptide receptor 3	2359	13.20	5.73×10^{-49}
MPEG1	macrophage expressed 1	219972	13.18	3.76×10^{-52}
LILRB2	leukocyte immunoglobulin like receptor B2	10288	13.14	4.39×10^{-34}
CD37	CD37 molecule	951	13.13	2.97×10^{-36}
LY86	lymphocyte antigen 86	9450	13.13	3.79×10^{-36}
PTPRC	protein tyrosine phosphatase receptor type C	5788	13.12	7.33×10^{-105}
SYK	spleen associated tyrosine kinase	6850	13.10	8.06×10^{-52}
CD48	CD48 molecule	962	13.10	5.13×10^{-39}
C1QB	complement C1q B chain	713	13.08	2.53×10^{-45}
C5AR1	complement C5a receptor 1	728	13.07	6.98×10^{-65}
ITGAM	integrin subunit alpha M	3684	13.06	4.76×10^{-62}
CCR5	C-C motif chemokine receptor 5 28gene/pseudogene29	1234	13.05	1.15×10^{-37}
GPR34	G protein-coupled receptor 34	2857	13.04	1.21×10^{-31}
MS4A7	membrane spanning 4-domains A7	58475	13.02	6.44×10^{-33}
HLA-DQB1	major histocompatibility complex2C class II2C DQ beta 1	3119	12.96	3.94×10^{-38}
LILRB1	leukocyte immunoglobulin like receptor B1	10859	12.95	1.70×10^{-48}
LRRC25	leucine rich repeat containing 25	126364	12.95	3.37×10^{-33}
AIF1	allograft inflammatory factor 1	199	12.94	2.79×10^{-48}
FCMR	Fc fragment of IgM receptor	9214	12.94	7.09×10^{-26}
ARHGAP30	Rho GTPase activating protein 30	257106	12.90	3.60×10^{-49}
IGSF6	immunoglobulin superfamily member 6	10261	12.89	1.58×10^{-66}
SCIMP	SLP adaptor and CSK interacting membrane protein	388325	12.85	1.41×10^{-31}
ALOX5	arachidonate 5-lipoxygenase	240	12.83	1.31×10^{-47}
TM4SF19	transmembrane 4 L six family member 19	116211	12.81	7.59×10^{-16}
GPNMB	glycoprotein nmb	10457	12.74	8.32×10^{-186}
CD300LF	CD300 molecule like family member f	146722	12.73	6.63×10^{-35}
SPN	sialophorin	6693	12.72	3.84×10^{-30}
PRKCB	protein kinase C beta	5579	12.70	9.81×10^{-32}
SMIM25	small integral membrane protein 25	100506115	12.69	2.56×10^{-35}
NFAM1	NFAT activating protein with ITAM motif 1	150372	12.68	1.54×10^{-47}
CSTA	cystatin A	1475	12.66	5.46×10^{-34}
KMO	kynurenine 3-monooxygenase	8564	12.62	2.21×10^{-35}
TLR8	toll like receptor 8	51311	12.60	3.87×10^{-33}
HK3	hexokinase 3	3101	12.59	2.46×10^{-64}
CYP1B1	cytochrome P450 family 1 subfamily B member 1	1545	12.58	1.09×10^{-72}
SIGLEC1	sialic acid binding Ig like lectin 1	6614	12.53	1.28×10^{-28}
IL2RG	interleukin 2 receptor subunit gamma	3561	12.52	2.34×10^{-70}
ITGB2	integrin subunit beta 2	3689	12.51	0.00
DNAJC5B	DnaJ heat shock protein family 28Hsp40 29 member C5 beta	85479	12.48	6.70×10^{-31}
LCP1	lymphocyte cytosolic protein 1	3936	12.48	8.00×10^{-124}
TREM2	triggering receptor expressed on myeloid cells 2	54209	12.48	2.30×10^{-75}
HAVCR2	hepatitis A virus cellular receptor 2	84868	12.47	3.32×10^{-90}
HLA-DMB	major histocompatibility complex 2C class II 2C DM beta	3109	12.46	2.94×10^{-119}
LPL	lipoprotein lipase	4023	12.46	5.21×10^{-33}
GPC4	glypican 4	2239	12.42	1.21×10^{-15}
MMP12	matrix metallopeptidase 12	4321	12.41	4.23×10^{-27}

tion, hematopoietic lineage and osteoclast differentiation in MAC when compared to HUVEC. As a next step, we compared our data to a previous microarray data set from the literature (Medina *et al*., 2010). A correlation analysis demonstrated that MAC show much stronger correlation with eEPC and monocytes than with OEC (Fig. 3**A**). Heatmaps of the respective gene lists as obtained from GOSTAT gene sets of endothelial cell development and

Table 5. Top 100 most differentially downregulated genes.

Gene	Name	Gene ID	log2FC	padj
NR2F2	nuclear receptor subfamily 2 group F member 2	7026	–13.59	1.97×10^{-39}
DKK1	dickkopf WNT signaling pathway inhibitor 1	22943	–13.28	1.50×10^{-34}
RHOJ	ras homolog family member J	57381	–12.60	1.55×10^{-44}
LAMA4	laminin subunit alpha 4	3910	–12.60	6.43×10^{-115}
ERG	ETS transcription factor ERG	2078	–12.53	5.68×10^{-48}
HHIP	hedgehog interacting protein	64399	–12.51	4.27×10^{-109}
MGP	matrix Gla protein	4256	–12.51	4.68×10^{-59}
TM4SF18	transmembrane 4 L six family member 18	116441	–12.50	3.17×10^{-29}
CLEC14A	C-type lectin domain containing 14A	161198	–12.44	3.31×10^{-81}
CCN2	cellular communication network factor 2	1490	–12.42	7.74×10^{-145}
ARHGEF15	Rho guanine nucleotide exchange factor 15	22899	–12.35	6.96×10^{-33}
NNMT	nicotinamide N-methyltransferase	4837	–12.33	7.90×10^{-35}
EFEMP1	EGF containing fibulin extracellular matrix protein 1	2202	–12.28	1.55×10^{-93}
ANGPT2	angiopoietin 2	285	–12.28	1.17×10^{-43}
MAP1B	microtubule associated protein 1B	4131	–12.20	1.94×10^{-54}
ADGRL4	adhesion G protein-coupled receptor L4	64123	–12.19	2.87×10^{-74}
PALMD	palmdelphin	54873	–12.04	1.45×10^{-42}
CDH5	cadherin 5	1003	–11.97	9.39×10^{-219}
PXDN	peroxidasin	7837	–11.96	1.94×10^{-128}
DIPK1B	divergent protein kinase domain 1B	138311	–11.94	1.55×10^{-53}
GJA1	gap junction protein alpha 1	2697	–11.93	3.62×10^{-112}
TAL1	TAL bHLH transcription factor 1 2C erythroid differentiation factor	6886	–11.93	1.99×10^{-31}
BGN	biglycan	633	–11.92	2.03×10^{-71}
MMRN1	multimerin 1	22915	–11.89	2.41×10^{-74}
MSRB3	methionine sulfoxide reductase B3	253827	–11.84	3.57×10^{-32}
COL4A1	collagen type IV alpha 1 chain	1282	–11.82	2.03×10^{-184}
COL8A1	collagen type VIII alpha 1 chain	1295	–11.73	1.29×10^{-50}
ESM1	endothelial cell specific molecule 1	11082	–11.69	3.03×10^{-45}
CLDN5	claudin 5	7122	–11.68	2.97×10^{-30}
PCDH10	protocadherin 10	57575	–11.68	1.12×10^{-39}
CCN1	cellular communication network factor 1	3491	–11.67	5.81×10^{-103}
ECSCR	endothelial cell surface expressed chemotaxis and apoptosis regulator	641700	–11.64	1.72×10^{-97}
ADGRF5	adhesion G protein-coupled receptor F5	221395	–11.61	4.39×10^{-29}
KIAA1549L	KIAA1549 like	25758	–11.55	4.04×10^{-30}
KIRREL1	kirre like nephrin family adhesion molecule 1	55243	–11.55	6.42×10^{-30}
ARHGAP29	Rho GTPase activating protein 29	9411	–11.54	4.57×10^{-117}
MFAP2	microfibril associated protein 2	4237	–11.54	5.30×10^{-27}
MMP16	matrix metallopeptidase 16	4325	–11.53	2.49×10^{-28}
LAMB1	laminin subunit beta 1	3912	–11.46	6.40×10^{-207}
EVA1A	eva-1 homolog A 2C regulator of programmed cell death	84141	–11.42	5.47×10^{-28}
SOX18	SRY-box transcription factor 18	54345	–11.42	1.60×10^{-25}
EDIL3	EGF like repeats and discoidin domains 3	10085	–11.38	1.44×10^{-27}
NFIB	nuclear factor I B	4781	–11.35	1.25×10^{-44}
VEGFC	vascular endothelial growth factor C	7424	–11.34	4.91×10^{-25}
COL12A1	collagen type XII alpha 1 chain	1303	–11.34	6.33×10^{-40}
FOXC2	forkhead box C2	2303	–11.32	2.52×10^{-24}
LIFR	LIF receptor subunit alpha	3977	–11.30	3.39×10^{-25}
ADGRL2	adhesion G protein-coupled receptor L2	23266	–11.27	1.88×10^{-36}
SEMA3F	semaphorin 3F	6405	–11.26	4.50×10^{-58}
BMP4	bone morphogenetic protein 4	652	–11.26	7.33×10^{-39}
EMCN	endomucin	51705	–11.26	2.12×10^{-47}
DIPK2B	divergent protein kinase domain 2B	79742	–11.24	6.86×10^{-39}

Table 5. Continued.

Gene	Name	Gene ID	log2FC	padj
SULF1	sulfatase 1	23213	–11.22	1.43×10^{-27}
SULT1E1	sulfotransferase family 1E member 1	6783	–11.16	2.45×10^{-18}
ROBO4	roundabout guidance receptor 4	54538	–11.16	9.68×10^{-107}
MYCT1	MYC target 1	80177	–11.16	1.55×10^{-78}
TMEM98	transmembrane protein 98	26022	–11.16	1.63×10^{-35}
MDFI	MyoD family inhibitor	4188	–11.14	9.85×10^{-26}
MEDAG	mesenteric estrogen dependent adipogenesis	84935	–11.12	1.62×10^{-27}
TMEM47	transmembrane protein 47	83604	–11.11	3.52×10^{-28}
AMOTL2	angiomotin like 2	51421	–11.09	1.02×10^{-44}
CHST1	carbohydrate sulfotransferase 1	8534	–11.09	3.58×10^{-24}
ESAM	endothelial cell adhesion molecule	90952	–11.08	4.01×10^{-97}
HOXA9	homeobox A9	3205	–11.03	2.83×10^{-26}
ADAMTS9	ADAM metallopeptidase with thrombospondin type 1 motif 9	56999	–11.03	8.54×10^{-25}
CYYR1	cysteine and tyrosine rich 1	116159	–10.98	4.28×10^{-23}
LTBP1	latent transforming growth factor beta binding protein 1	4052	–10.95	1.08×10^{-61}
NR2F1	nuclear receptor subfamily 2 group F member 1	7025	–10.94	2.27×10^{-26}
ADAMTS18	ADAM metallopeptidase with thrombospondin type 1 motif 18	170692	–10.90	3.04×10^{-23}
HOXA10-HOXA9	HOXA10-HOXA9 readthrough	100534589	–10.89	9.53×10^{-26}
GPR4	G protein-coupled receptor 4	2828	–10.89	1.22×10^{-25}
GNG11	G protein subunit gamma 11	2791	–10.89	5.29×10^{-207}
CAV1	caveolin 1	857	–10.84	9.46×10^{-293}
ANXA3	annexin A3	306	–10.83	9.60×10^{-32}
MARCHF4	membrane associated ring-CH-type finger 4	57574	–10.83	2.02×10^{-23}
GULP1	GULP PTB domain containing engulfment adaptor 1	51454	–10.77	4.33×10^{-25}
VEPH1	ventricular zone expressed PH domain containing 1	79674	–10.77	1.50×10^{-43}
C1QTNF5	C1q and TNF related 5	114902	–10.76	1.55×10^{-24}
MFRP	membrane frizzled-related protein	83552	–10.76	1.55×10^{-24}
SCARA3	scavenger receptor class A member 3	51435	–10.76	7.91×10^{-50}
HTR1B	5-hydroxytryptamine receptor 1B	3351	–10.74	1.33×10^{-24}
FAT4	FAT atypical cadherin 4	79633	–10.74	5.29×10^{-30}
OSMR	oncostatin M receptor	9180	–10.73	8.70×10^{-23}
RARB	retinoic acid receptor beta	5915	–10.72	4.08×10^{-24}
MECOM	MDS1 and EVI1 complex locus	2122	–10.70	4.96×10^{-44}
NOVA2	NOVA alternative splicing regulator 2	4858	–10.66	8.01×10^{-25}
ADAMTSL1	ADAMTS like 1	92949	–10.66	1.17×10^{-20}
PTPRB	protein tyrosine phosphatase receptor type B	5787	–10.63	1.15×10^{-95}
MEOX2	mesenchyme homeobox 2	4223	–10.63	4.10×10^{-23}
TCIM	transcriptional and immune response regulator	56892	–10.62	5.92×10^{-22}
CNTNAP3	contactin associated protein like 3	79937	–10.55	3.47×10^{-24}
GJA1P1	gap junction protein alpha 1 pseudogene 1	2698	–10.55	1.00×10^{-24}
CNN3	calponin 3	1266	–10.54	2.15×10^{-134}
FBXL7	F-box and leucine rich repeat protein 7	23194	–10.54	5.24×10^{-25}
CDH2	cadherin 2	1000	–10.50	1.50×10^{-44}
TBX18	T-box transcription factor 18	9096	–10.47	2.59×10^{-24}
SOX17	SRY-box transcription factor 17	64321	–10.47	1.82×10^{-22}
HMGA2	high mobility group AT-hook 2	8091	–10.46	1.12×10^{-71}
CDH13	cadherin 13	1012	–10.43	1.10×10^{-71}
MYRIP	myosin VIIA and Rab interacting protein	25924	–10.43	1.67×10^{-21}

macrophage differentiation are shown in Fig. 3**B,C**. These results demonstrate a remarkable similarity between the published early EPC data (Medina *et al.*, 2010) and our MAC population, which both show a high similarity to the published monocyte transcriptome. The published late outgrowth endothelial cell (OEC) signature in contrast showed

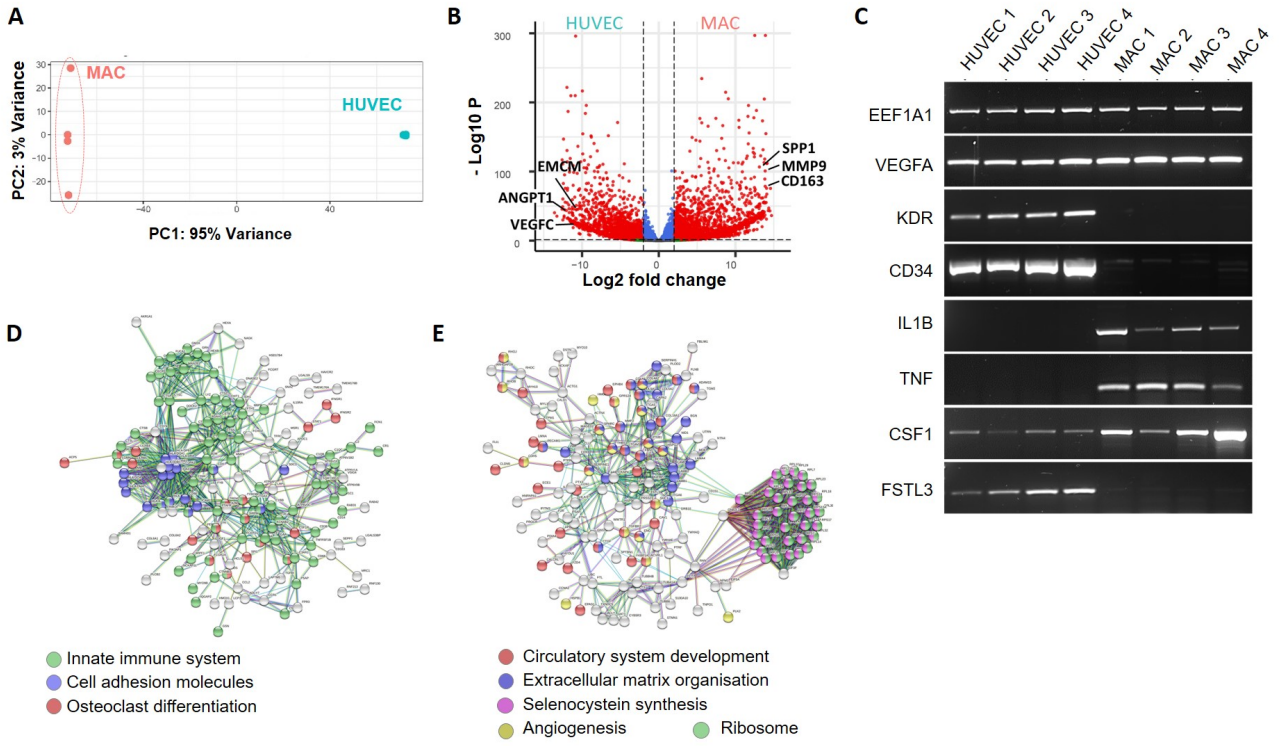

Fig. 2. Gene signature of CYR61-enriched MAC. RNAseq analysis was performed on CYR61-enriched MAC (n = 4 donors) and HUVEC (RNA collected from 4 independent experiments). (**A**) Principle component analysis showing clear separation of the two cell populations, where PC1 accounts for 95 % of variance. As expected MAC show donor dependent variance, as seen by a 3 % variance in PC2. (**B**) Volcano plot representation of the most significant regulated genes between HUVEC and MAC. Positive fold changes refer to differentially upregulated genes in MAC, which include several typical macrophage marker while endothelial marker were more highly expressed in HUVEC. (**C**) RT-PCR was performed to validate gene expression pattern observed in RNA-seq. Results of four different samples referring to HUVEC collected from four independent experiments and MAC isolated from 4 different donors are shown. (**D,E**) String pathway analysis with the 250 most highly regulated genes in MAC (**D**) and HUVEC (**E**) indicating clustering in typical innate immune cell and endothelial pathways, respectively.

similarity with the HUVEC signature in all profiles shown, indicating that our MAC population resembles the published early EPCs (eEPC) that is different to late OEC with EC characteristics. Of note, the gene expression profile of our MAC population as well as previously identified eEPC populations in part also reflects the cellular response to the adhesion to extracellular matrix compounds, in our case CYR61.

CYR61-enriched MAC Show Typical Monocyte/Macrophage Features and Have the Ability to Develop a Multinucleated Osteoclast-like Phenotype

To further test monocyte/macrophage-related features of MAC, we applied a typical protocol for macrophage differentiation and polarization and compared results between cells seeded on standard tissue culture plastic (TCP) and CYR-61 coating (Fig. 4). Treatment with LPS induced a strong shift towards a CD80+/CD86+ double positive population without significant differences between CYR61-coating and TCP (Fig. 4**A,B**), which was accompanied by a trend for upregulation of *IL6* and *IL1B* gene expressing (Fig. 4**E**). Next, we tested a one day IL-4 treatment for the induction of an anti-inflammatory M2-like macrophage phenotype but did not observe significant differences in *CD163* or *CD206* expression in flow cytometry or qPCR (Fig. 4**D,E**).

Interestingly, in long term cultures as well as in media containing osteoclastogenic, but also endothelial factors, multinucleated giant cells appeared, partly resembling a Langhans pattern of nuclei arrangement, after 2–3 weeks of culture (Fig. 5**A**). In the presence of a classical regimen of osteoclast differentiation *in vitro* using M-CSF/RANKL as initiators a relatively homogenous population of osteoclast-like partly multinucleated cells developed (Fig. 5**A**), very similar to the results seen with a mononuclear fraction of cells harvested from buffy coats without CYR61, used as a positive control for classical OC differentiation (data not shown). Cell populations differentiated with classical osteoclast differentiation protocols expressed calcitonin receptors (*CALCR*), *TRAP*, and *CTSK* along with *MMP-9*, *SSP1* and *CD31* (Fig. 5**A,B,D**). Upon addition of RANKL in the last step of osteoclastic differ-

Table 6. KEGG Pathway analysis.

Description	NES	qvalues	setSize
Antigen processing and presentation	2.4784	0.0065	70
Hematopoietic cell lineage	2.3831	0.0065	92
Allograft rejection	2.2862	0.0065	35
Osteoclast differentiation	2.2791	0.0065	124
Primary immunodeficiency	2.2634	0.0065	38
B cell receptor signaling pathway	2.2465	0.0065	79
Natural killer cell mediated cytotoxicity	2.2421	0.0065	112
Systemic lupus erythematosus	2.2377	0.0065	123
Rheumatoid arthritis	2.2266	0.0065	89
Viral protein interaction with cytokine and cytokine receptor	2.2178	0.0065	94
Th17 cell differentiation	2.1929	0.0065	102
NF-kappa B signaling pathway	2.1374	0.0065	103
T cell receptor signaling pathway	2.1159	0.0065	102
Chemokine signaling pathway	2.0781	0.0065	183
Th1 and Th2 cell differentiation	2.0716	0.0065	87
Toll-like receptor signaling pathway	2.0221	0.0065	90
Cytokine-cytokine receptor interaction	1.9811	0.0065	255
NOD-like receptor signaling pathway	1.9199	0.0065	155
Complement and coagulation cascades	1.8440	0.0065	75
Toxoplasmosis	1.8332	0.0065	110
C-type lectin receptor signaling pathway	1.7946	0.0065	101
Cell adhesion molecules (CAMs)	1.7480	0.0065	136
Fc gamma R-mediated phagocytosis	1.7385	0.0065	90
PD-L1 expression and PD-1 checkpoint pathway in cancer	1.7361	0.0065	88
Fc epsilon RI signaling pathway	1.7214	0.0065	63
Necroptosis	1.6769	0.0065	143

KEGG, Kyoto Encyclopedia of Genes and Genomes.

entiation, NANOG expression disappeared and *CD14* expression was reduced (Fig. 5**D**). Flow cytometry analysis after OC differentiation protocols showed a relatively homogenous population with typical monocyte/macrophage features, i.e., CD11b+/acLDL+ (Fig. 5**C**).

CYR61-enriched MAC do not by Themselves Build Angiogenic Networks and Participate in Angiogenic HUVEC Networks

Since the discussion about participation of EPC populations in neoangiogenesis is ongoing, we performed Matrigel angiogenesis assays using MAC alone and in co-culture with HUVEC. As expected, HUVEC formed a cellular network within the first 24 h of incubation (Fig. 6**A–C**) as observed in previous studies (Herrmann *et al*., 2016). There was no evidence for network formation when using MAC alone Fig. 6**G–I**). Co-culture experiments using a combination of pre-stained MAC and HUVEC showed participation of single fluorescent MAC in networks established by HUVEC (Fig. 6**D–F**).

Cocultured CYR61-enriched MAC and Their Supernatants Inhibit Mineralization of Primary Skeletal Precursor Cells (MSC) during in Vitro Osteogenic Differentiation Protocols

A tight interaction between endothelial cells and bone formation processes has been previously reported *in vivo* and *in vitro* (Bouland *et al.*, 2021). Since the role of MAC is currently less clear, we here tested the influence of CYR61-enriched MAC on *in vitro* mineralization of primary bone marrow-derived MSC. In the first two experimental groups MSC were expanded and cultured in osteogenic media for 14 days. By this time point CYR61-enriched MAC or MAC-conditioned medium were added or not on top of the differentiating monolayers (Fig. 7**A**). After another 14 days (28 days of differentiation) mineralization, semi-quantitatively measured by Alizarin Red staining, was markedly inhibited (Fig. 7**B,C** left and middle panels). Similar effects could be achieved when MSC were differentiated in the presence of MAC-conditioned medium for the entire 28-day period (Fig. 7**A–C**, right panel). The inhibiting effects on mineral deposition without touching markers of osteogenic differentiation could be confirmed by analysis of typical osteogenic marker genes, namely *Runx2*, alkaline phosphatase (*ALPL*) and bone sialoprotein (*IBSP*),

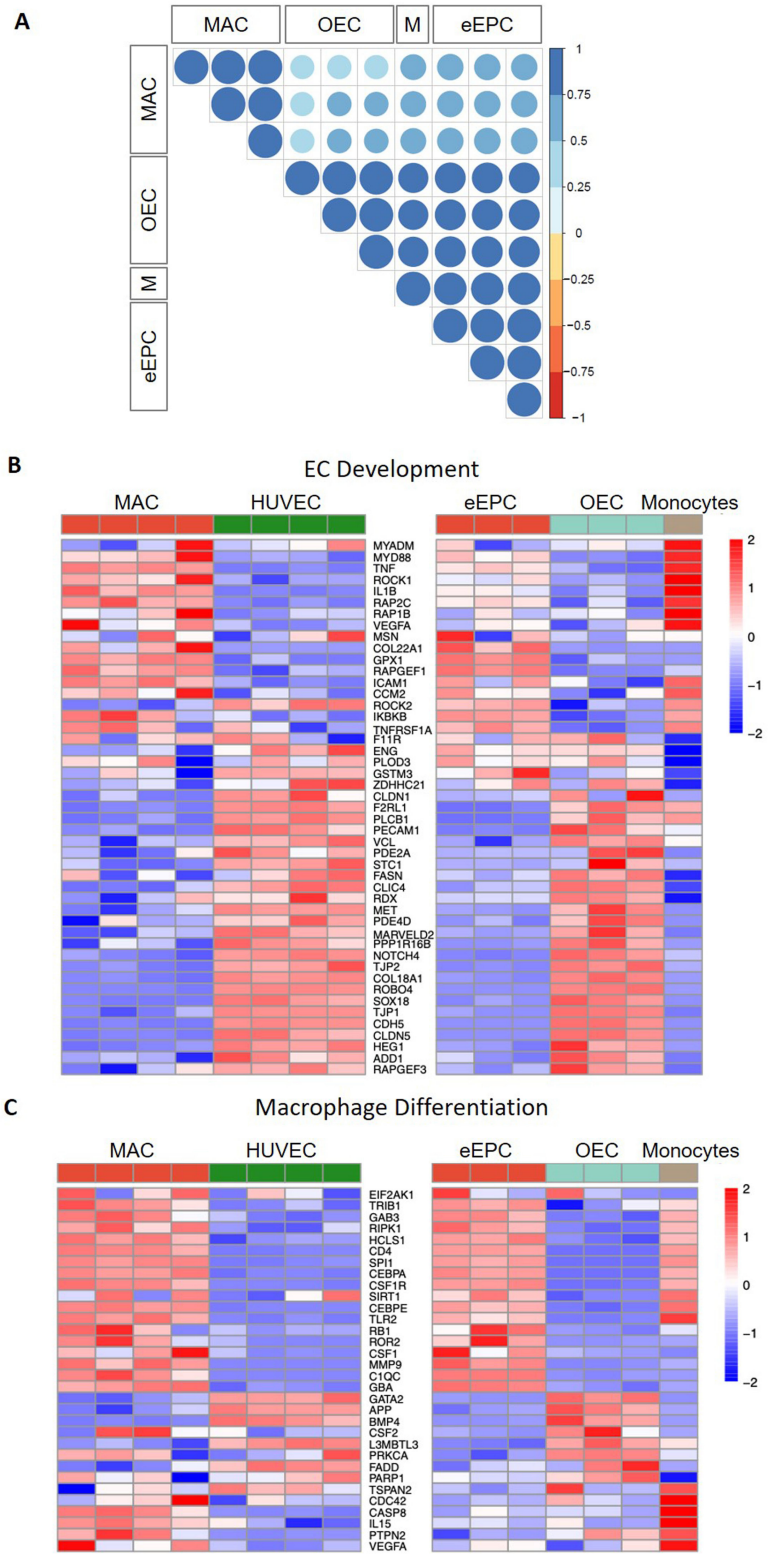

Fig. 3. Comparison of CYR-enriched MAC with other myeloid and endothelial cell populations. (**A**) Spearmann correlation calculated by comparing our RNAseq data set and log transformed microarray data on early EPC (eEPC), outgrowth endothelial progenitor cells (OEC) and monocytes retrieved from (Medina *et al*., 2010). Color intensity and the size of the circle are proportional to the correlation coefficients. In the right side of the plot, the legend color shows the correlation coefficients and the corresponding colors with the values ranging from – 1 to + 1. (**B,C**) Comparative heatmap analysis for genes related to (**B**) EC development and (**C**) macrophage differentiation in CYR-enriched MAC and compared with other myeloid and endothelial cell populations. Data shows high similarity between MAC and eEPC.

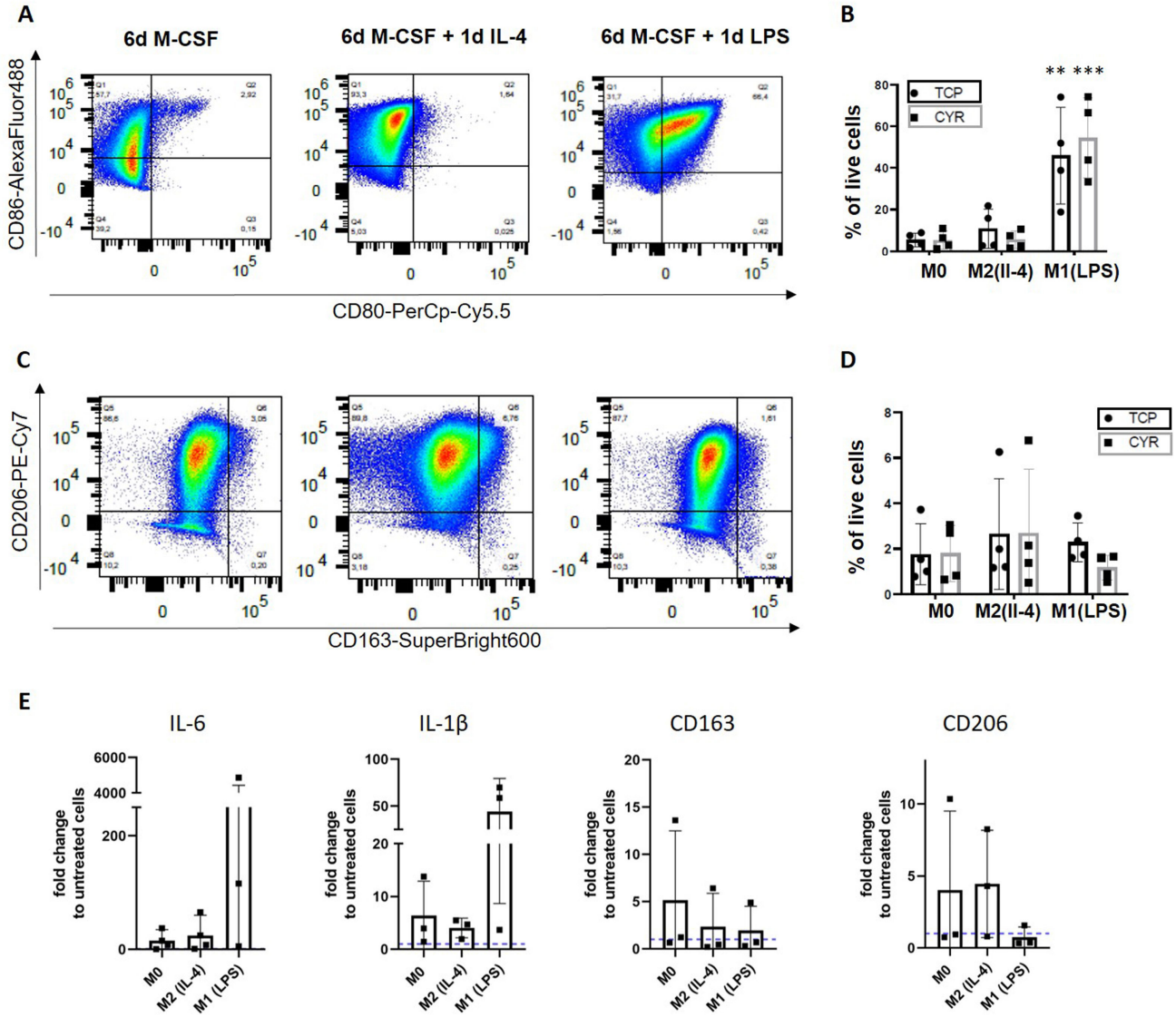

Fig. 4. Influence of CYR61 coating on macrophage differentiation and polarization. A protocol for macrophage differentiation and polarization towards a M1 or M2 phenotype was adopted for MNC seeded on either tissue culture plastic (TCP) or CYR61-coated plates. (**A**) Representative flow cytometry results for M1 macrophage markers at day 7 for the CYR61 group, indicating a high percentage of CD86+CD80+ cells in the LPS stimulated group that was confirmed by quantification (**B**) for both TCP and CYR61. Two-way ANOVA with Tukey's Multiple Comparison Test was applied to test for statistical significance. **, $p < 0.01$ and ***, $p < 0.001$ both to all other groups. (**C**) Representative flow cytometry results for M2 macrophage markers at day 7 for the CYR61 group. Only minor changes were detected between groups, with a trend of slightly higher CD206+ and CD206+/CD163+ cell populations upon IL4 stimulation in some donors but not all (**D**). (**E**) qPCR gene expression analysis was performed with cells of three donors cultured on CYR61-coated plates. High donor variability was seen between donors but there is a clear trend of increased expression of pro-inflammatory markers IL6 and IL1β upon LPS stimulation and CD206 appeared to expressed to a higher level in cells treated with M-CSF only or additionally with IL4. qPCR was performed in triplicates and values were calculated with the $\Delta\Delta$Ct method and normalized to the respective untreated control (dashed line). *RPLP0* was used as housekeeping gene. Kruskal-Wallis test (IL6, CD206) or ordinary one-way ANOVA (IL1β, CD163) was applied to test for statistical significance.

where only a trend of lower expression was seen for IBSP in comparison to MSC cultured alone (Fig. 7**D**).

Discussion

We describe here in depth with functional end point analyses a population of cells in the peripheral blood which can be efficiently enriched on plates that are coated with CYR61 matricellular protein as published in earlier work

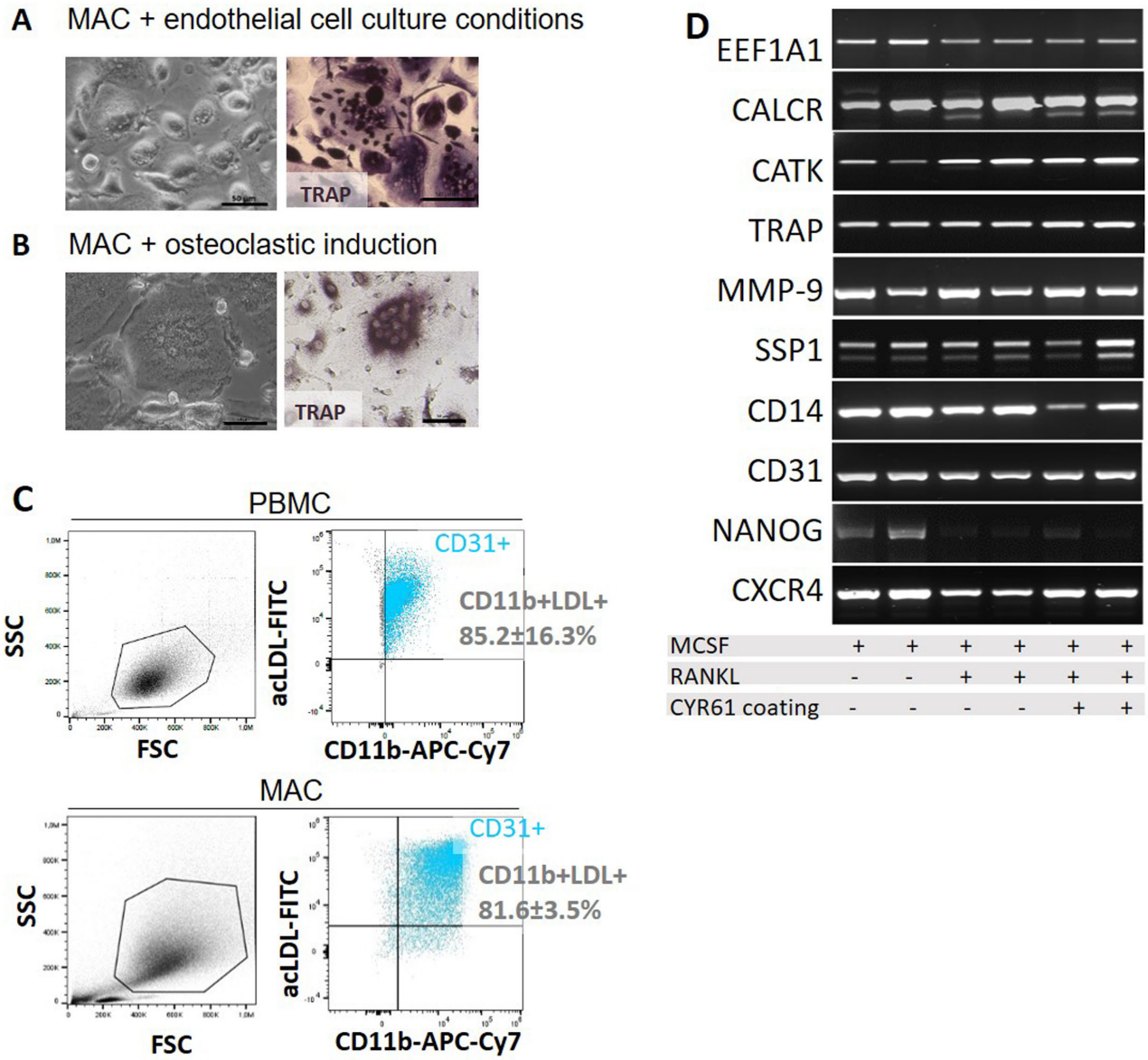

Fig. 5. Osteoclastic differentiation of CYR-61 enriched MAC. (**A,B**) Spontaneous development of TRAP-positive multinucleated osteoclasts-like cells in MAC cultured for two weeks in endothelial differentiation medium. (**B**) TRAP-positive multinucleated cells are detected after culture of MAC in osteoclastic induction media (MCSF/RANKL). (**C**) Flow cytometry of CYR61-enriched MAC or PBMC (control) after culture in osteoclast induction medium. Both cultures retrieve a homogenous cell population as seen in FSC/SSC plots, showing high positivity for CD11b and CD31 and the ability for uptake of acLDL particles. Mean percentages of positive cells in the entire population and standard deviation of 4 donors are presented. (**D**) RT-PCR analysis of CYR61-enriched MAC or control cells after MCSF/RANKL treatment shows that RANKL enhances preexisting expression of calcitonin receptor (*CALCR*) while expression of stemness marker *NANOG* is abolished. No obvious differences are observed between the full PBMC population or CYR-61 selected MAC, except slightly reduced expression of the monocytic marker *CD14*. Depicted are representative results from two cell preparations.

by our group (Hafen *et al*., 2018). The *in vitro* enrichment strategy mimics the process of CYR61-guided adhesion of "patrolling" monocytic cells to endothelial cells (Imhof *et al*., 2016) and thus helps in expanding our knowledge of the characteristics of the attaching MAC population with implications for the endogenous repair process. The enriched cell population largely resembles cells that have been described and classified as "early endothelial precursor cells", circulating angiogenic cells (CAC) or paracrine endothelia cells (PAC) because of their similarities in surface markers and acLDL uptake (Basile and Yoder, 2014; Chopra *et al*., 2018; Medina *et al*., 2010; Rehman *et al*., 2003; Shi *et al*., 2014). Upon characterization, the enriched population (albeit still heterogeneous) besides some characteristics of endothelial precursors shows more monocyte/macrophage like attitudes. The cells harbor some features of progeni-

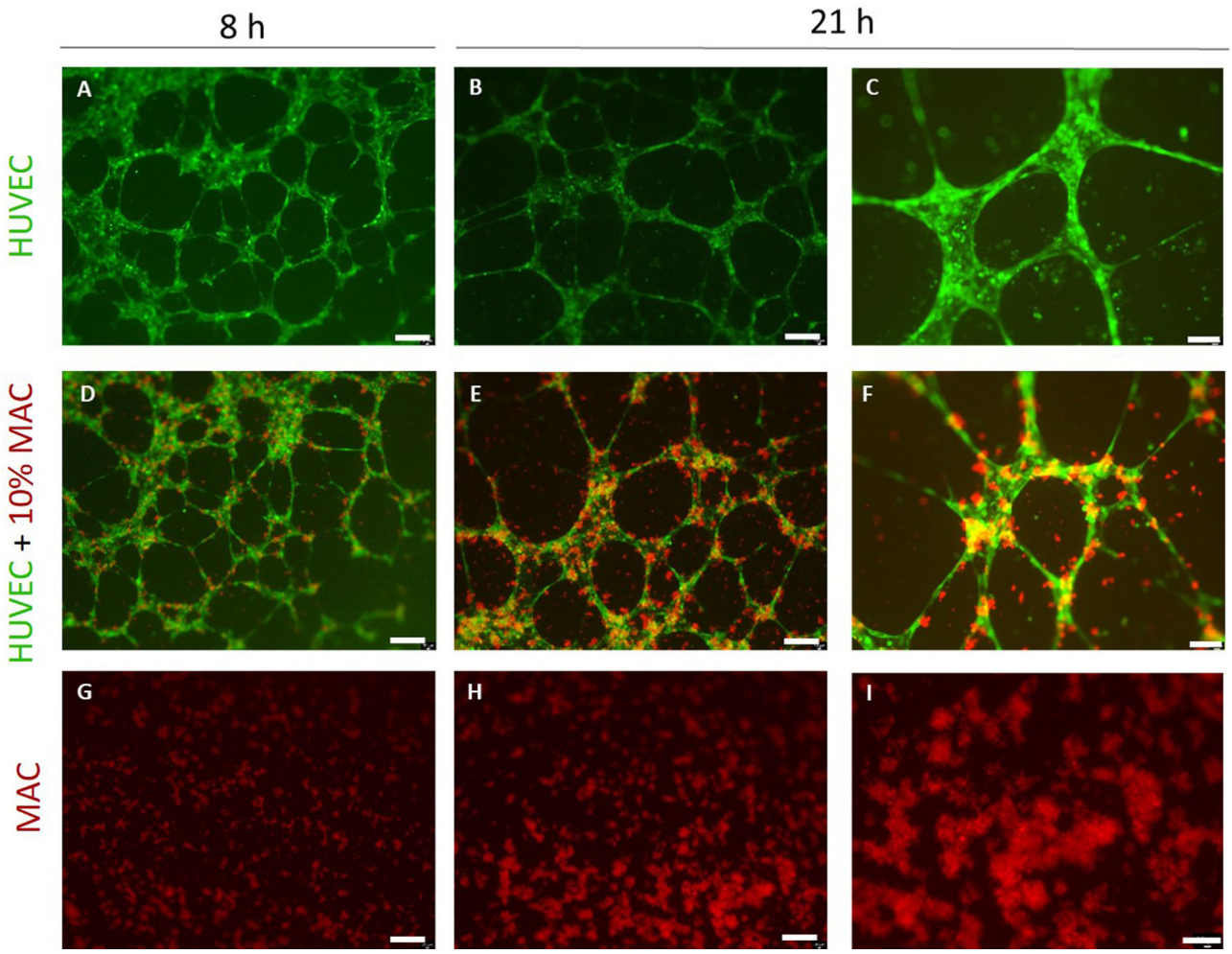

Fig. 6. CYR61-enriched MAC contribute to network formation on Matrigel. A Matrigel assay was performed to assess the angiogenic potential of Cyr61-enriched cells. After 7 days of culture MAC were collected from CYR61-coated plates, labeled with cell tracker red and cultured in single (**G–I**) or co-cultures (**D–F**; HUVEC:MAC ratio 9:1) on Matrigel, HUVEC single cultures served as control (**A–C**). Network formation was assessed by fluorescence microscopy after 8 h and 21 h. Scale bar depicts 200 µm (**A,B,D,E,G,H**) and 100 µm (**C,F,I**).

tor cells in that they express marker genes that are associated with stemness (e.g., *OCT4, SOX2, NANOG*) and stem cell niches (e.g., *CXCR4*) and can be developed *in vitro* towards macrophage- and osteoclast-like multinucleated phenotypes thereby generating a much more homogenous population (Fig. 5**C**). Moreover, polarization experiments yield M1 macrophages after treatment with LPS (Fig. 4). Although not capable of performing angiogenic networks on their own, MAC perform as participants in networks in Matrigel-assays together with HUVEC. These findings are in line with previous literature, where early EPC populations were identified as MAC/CAC that support angiogenesis by secretion of paracrine factors (Chambers *et al*., 2018; Grunewald *et al*., 2006; Shi *et al*., 2014). This is also consistent with an adaptive increase in their numbers in scenarios with increased demand for neoangiogenesis, e.g., vascular injury (Kapoor *et al*., 2021) or exercise (Landers-Ramos *et al*., 2019). Common protocols for purification of MAC rely on cell adherence on fibronectin or collagen coated plates. In contrast, we here apply CYR61-coating in order to resemble a situation of monocytic cell adhesion to endothelia (Hernandez and Iruela-Arispe, 2020; Imhof *et al*., 2016; Wolf *et al*., 2019). This results in significantly higher cell enrichment efficiency compared to fibronectin coating, which may be the consequence of attracting a patrolling subset of monocyte precursors. Upon characterization of surface markers such as CD14, CD31, CD11b or LDL uptake capacity, we do not find significant differences between fibronectin-enriched and CYR61-enriched populations.

In order to further characterize this population, we performed RNA-seq based transcriptome signature analysis in comparison with HUVEC and other publicly available transcriptomes of regenerative populations (Medina *et al*., 2010). We find signatures that in part resemble both endothelial and monocyte characteristics, but certainly no true

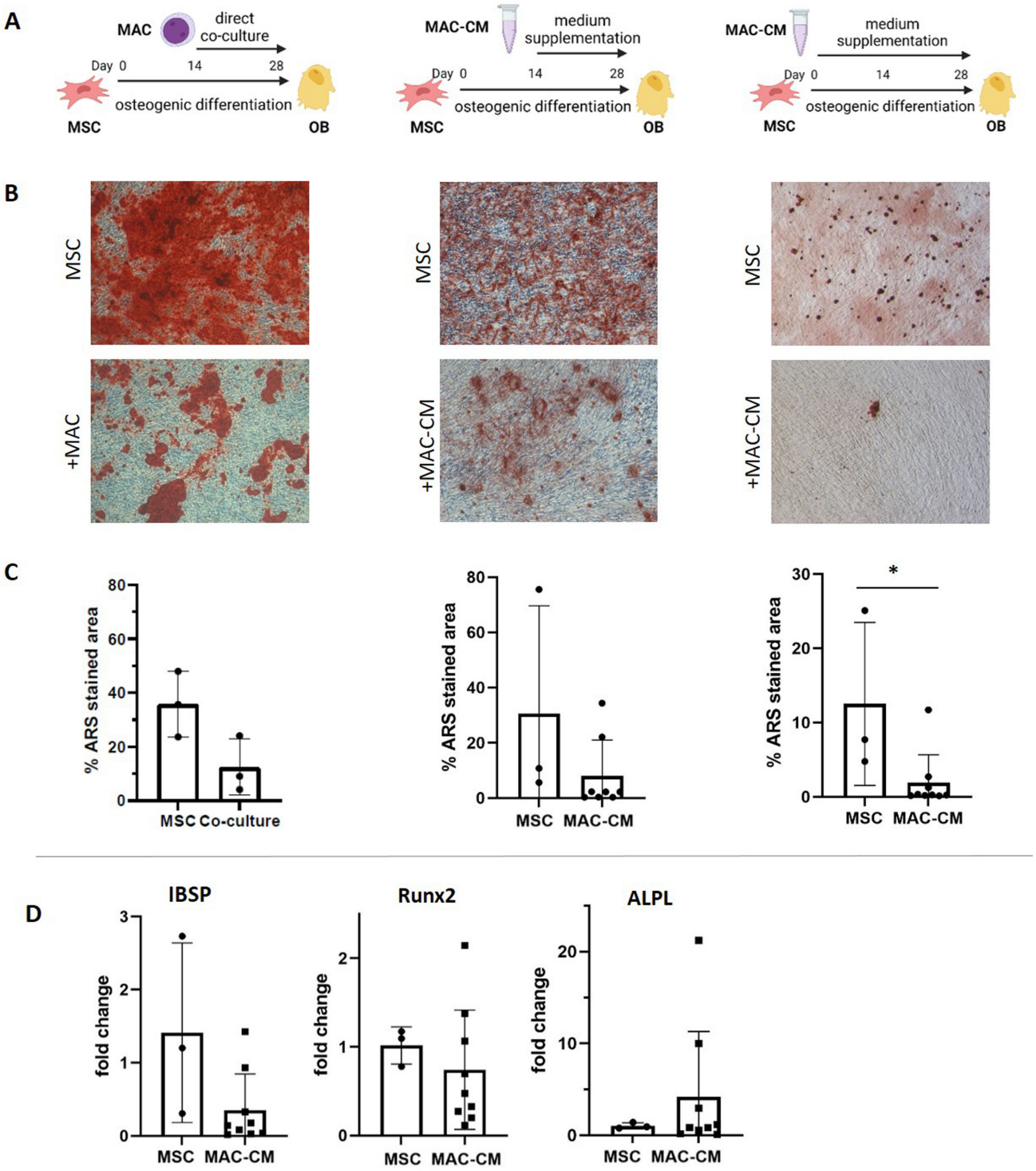

Fig. 7. MAC or their supernatants inhibit osteogenic differentiation of MSC *in vitro*. (**A**)Experimental set-up and (**B**) representative images of Alizarin Red S (ARS) mineral staining after 28 days of osteogenic differentiation of MSC alone, in direct co-culture with MAC or with MAC conditioned medium (CM) as indicated. Scale bar = 100 µm. (**C**) Quantification of the ARS-stained area of the well plate, indicating reduced mineral deposition in all groups with MAC or MAC-CM. An upaired *t*-test or Mann-Whitney test was applied to test for statistical significance for normally or not-normally distributed data, respectively. * $p < 0.05$. (**D**) Gene expression analysis of typical osteogenic markers after 28 days. Controls refer to MSC cultured alone, RPLP0 was used as housekeeping gene and values were calculated with the ΔΔCt method; all samples were run in triplicates. Wilcoxon Signed Rank statistics was applied. CM from three MAC donors were tested on two different MSC donors.

mature endothelial signatures, indicating that we enrich a highly plastic myeloid cell population that is mobilized to the peripheral blood circulation and can support angiogenesis, inhibit calcification *in vitro* and can be differentiated towards macrophages that adopt a multinucleate phenotype including an osteoclast like one. We found large similarities between our CYR61-enriched MAC and published eEPC/MAC/CAC populations obtained by enrichment on fibronectin-coated plates (Medina *et al.*, 2010). These cells have been described as a population with pro-angiogenic M2 macrophage characteristics supporting angiogenesis via IL-8 secretion and thus utilizing strong tissue repair potential (Medina *et al.*, 2010). In line with this, transcriptomic analysis of CAC has confirmed a macrophage genotype with features of M2 regulatory tissue macrophages (Everaert *et al*., 2019). In accordance, we here found in our RNA-seq analysis that MAC express markers of M2 polarization such as *CD163*, *MRC1*, *CD206*, *dectin-1/CLEC7A* (as described in (Pireaux *et al*., 2021)), and some other CD marker molecules such as *CD74*, *CD68*, *CD84* and *CD14*. Moreover, MAC also express some genes described in alternatively activated M2 macrophages (as reported in (Orecchioni *et al*., 2019)), such as *MRC1*, *FLT1*, *CLEC7a*, *CLEC10a*, *OCSTAMP*, *PTGS2*. Since M2 macrophages stimulate angiogenesis, their participation in our angiogenesis assay would be in line and this population should further be tested as to its role in tissue engineering and *in vivo* regeneration (Hong and Tian, 2020; Schlundt *et al*., 2018; Spiller *et al*., 2015).

Circulating monocytes/macrophages derived from granulocyte/macrophage precursors (GMP) migrate from bone marrow into the circulation and are consecutively distributed into different tissues where they support/replenish tissue associated or resident macrophages (reviewed in (Wolf *et al*., 2019) and (Varol *et al*., 2015)). Circulating monocytes are an extremely heterogeneous population as they can be both derived from GMP and monocyte-dendritic cell progenitors (MDP) and become classical, intermediate and non-classical monocytes, which again may be selected into at least eight identifiable subpopulations (reviewed in (Wolf *et al*., 2019)). The population we enriched here expresses CXCR4, which is typically expressed in the stem cell niche and may be indicative that MAC were only recently released from the bone marrow, because this feature is lost as they mature. Being both positive for CD14 and CD16 the majority of cells may also represent an intermediate phenotype that rapidly changes in culture and upon differentiating stimuli. Nevertheless, it appears that upon strong stimulation they can be pushed towards more homogenous populations like M1 macrophage-like cells (Fig. 4).

Remarkably strong expression of osteopontin (*SPP1*) is another surprising hallmark of CYR61-enriched MAC, as it was recently described for various myeloid/macrophage subpopulations like tumor associated macrophages, a subpopulation in the liver, and reparative macrophages in the heart after myocardial infarction (Schlecht *et al*., 2021; Tardelli *et al*., 2016). Osteopontin (OPN) strongly inhibits mineralization. This function is dependent on polypeptide phosphorylation of the protein driven by tissue non-specific alkaline phosphatase (TNSALP) (Maniatis *et al*., 2020; Sabbah *et al*., 2019). In line with this, osteoblast cultures derived from OPN-deficient mice show increased mineralization *in vitro* (Holm *et al*., 2014). Likewise, increased OPN level in FGF23-deficient animals have been shown to contribute to the osteomalacia phenotype in these animals (Yuan *et al*., 2014). OPN also binds to hydroxyapatite with high affinity and is involved in the attachment of osteoclasts to the mineralized bone matrix. Recent research has assigned quite a few additional functions to OPN in stem cell biology, inflammation and cancer and especially also in angiogenesis and vascular biology and pathology (Wing *et al*., 2020; Bouleftour *et al*., 2017). OPN was traditionally looked upon as a bone protein, mainly expressed by bone forming cells, but this is also true for subsets of macrophages which is in line with our finding (Bai *et al*., 2020); (Anisiewicz *et al*., 2020; Schlecht *et al*., 2021; Tardelli *et al*., 2016; Vianello *et al*., 2020). Taken together, these findings suggest that OPN secretion may account for important functional properties of CYR61-enriched cells as we could show for the inhibition of mineralization of MSC on their way to become osteoblasts. In light of the additional functions of OPN, e.g., in inflammation, the role of OPN secretion by MAC in the process of tissue regeneration and inflammation in humans remain to be dissected.

The relationship between myeloid cells and particularly bone marrow residing macrophages, osteomacs, and skeletal progenitors has also been studied in the context of bone homeostasis and remodeling where pro-osteogenic effects of osteomacs have been described (Ponzetti and Rucci, 2019). This seems like an apparent contrast to our results of inhibited mineral deposition during *in vitro* osteogenesis in MSC monolayer cultures in presence of this MAC population that might be related to the secretion of OPN. However, given that polypeptides derived from OPN may serve opposite task upon minimal post translational changes like dephosphorylation by variably expressed alkaline phosphatase, an explanation might not be as far fetched as it seemingly is. Further studies, in particular *in vivo*, will have to be performed to elucidate the role of the MAC population CYR61-enriched cells in bone formation and tissue regeneration.

Conclusions

In summary, we describe here the population of circulating precursor cells previously discussed as “early EPC” as a monocytic cell population with high plasticity that should better be called MAC as suggested in previous work. The scientific community is quite in agreement that peripheral blood monocytes cells consist of an array of different

subpopulation with high plasticity both with respect to the various phenotypes of the monocyte/macrophage lineage and the plethora of their functional profiles in inflammation and regeneration. The mechanism of blood cell attachment to CYR61 has been described *in vivo* in the context of different leukocytes and specifically monocyte populations and their recruitment to sites of vascular inflammation (Imhof *et al*., 2016; Löbel *et al*., 2012). In this context, our data makes a significant contribution towards a better characterization of this particular cell population. We conclude that there is an urgent need to further dissect this functional profile in regenerative environments in health and disease. Such data would also guide potential therapeutic applications of CYR61-enriched cells or the incorporation of CYR61-coating in biomaterial designs to support early events in tissue healing and regeneration.

List of Abbreviations

EPC, endothelial progenitor cells; MAC, myeloid angiogenic cells; MSC, mesenchymal stromal cells; EC, endothelial cells; CAC, circulating angiogenic cells; ECFC, endothelial colony forming cells; OEC, outgrowth endothelial cells; EMPs, Erythro-myeloid progenitors; ECM, extracellular matrix; TSP-1, thrombospondin-1; TN-C, tenascin-C; SPP1, osteopontin; VEGF, vascular endothelial growth factor; rCYR61, recombinant CYR61-protein; PBS, phosphate buffered saline; PBMC, Peripheral Blood Mononuclear Cells; FBS, fetal bovine serum; RT, room temperature; MNC, mononuclear cells; LPS, lipopolysaccharides; qPCR, Quantitative PCR; RPLP0, ribosomal protein, large, P0; acLDL, acetylated low density lipoprotein; HUVEC, Human umbilical vein endothelial cells; KEGG, Kyoto Encyclopedia of Genes and Genomes; OCT4, octamer binding transcription factor 4; SOX2, SRY (sex determining region Y)-box 2; VCAM, vascular cell adhesion molecule; TIE1, tyrosine kinase with immunoglobulin like and EGF like domains 1; KDR, vascular endothelial growth factor receptor 2; FLT1, vascular endothelial growth factor receptor 1; SPP1, secreted phosphoprotein 1; OPN, osteopontin; EMCN, endomucin; ANGPTL4, angiopoietin like 4; VWF, von Willebrand factor; FN, fibronectin; CM, conditioned media; eEPC, early EPC; TCP, tissue culture plastic; CALCR, calcitonin receptors; CTSK, cathepsin K; ALPL, alkaline phosphatase; IBSP, bone sialoprotein; ARS, Alizarin Red S; PAC, paracrine endothelia cells; GMP, granulocyte/macrophage precursors; MDP, monocyte-dendritic cell progenitors; TNSALP, tissue nonspecific alkaline phosphatase.

Availability of Data and Materials

Data are available upon request from the corresponding author, MH.

Author Contributions

Contributions in detail: MH: Conceptualization, Methodology, Investigation, Data curation, Resources, Writing - Original Draft, Funding acquisition; JS: Methodology, Investigation, Writing – Review & Editing; SW: Methodology, Investigation, Writing – Review & Editing; MK: Methodology, Investigation, Writing – Review & Editing; MR: Resources, Writing – Review & Editing; ML: Resources, Writing – Review & Editing; MS: Methodology, Data curation, Writing – Review & Editing; NS: Methodology, Writing – Review & Editing, Supervision; RE: Methodology, Writing – Review & Editing, Supervision, Funding acquisition; DD: Resources, Writing – Review & Editing, Supervision; FJ: Conceptualization, Resources, Data curation, Writing - Original Draft, Supervision. All authors contributed to editorial changes in the manuscript, read and approved the final manuscript, and have participated sufficiently in the work to take public responsibility for appropriate portions of the content.

Ethics Approval and Consent to Participate

The isolation of bone marrow MSC from residual material from orthopedic patients undergoing hip replacement surgery was approved by the local Ethics Committee of the University of Würzburg (permission number 186/18).

Acknowledgments

Not applicable.

Funding

M.H. is supported by the Interdisciplinary Center for Clinical Research (IZKF) at the University of Würzburg (Project D-361). This study was supported by the Europäischer Fonds für regionale Entwicklung (EFRE) grant EU-1650-0006. This publication was supported by the Open Access Publication Fund of the University of Wuerzburg.

Conflict of Interest

The authors declare no conflict of interest. DD is serving the Editorial Board members of this journal. We declare that DD had no involvement in the peer review of this article and has no access to information regarding its peer review. Full responsibility for the editorial process for this article was delegated to JG.

References

Anisiewicz A, Łabędź N, Krauze I, Wietrzyk J (2020) Calcitriol in the Presence of Conditioned Media from Metastatic Breast Cancer Cells Enhances Ex Vivo Polarization of M2 Alternative Murine Bone Marrow-Derived Macrophages. Cancers 12: 3485. DOI: 10.3390/cancers12113485.

Asahara T, Murohara T, Sullivan A, Silver M, van der Zee R, Li T, Witzenbichler B, Schatteman G, Isner JM

(1997) Isolation of putative progenitor endothelial cells for angiogenesis. Science (New York, N.Y.) 275: 964-967. DOI: 10.1126/science.275.5302.964.

Avraham-Davidi I, Yona S, Grunewald M, Landsman L, Cochain C, Silvestre JS, Mizrahi H, Faroja M, Strauss-Ayali D, Mack M, Jung S, Keshet E (2013) On-site education of VEGF-recruited monocytes improves their performance as angiogenic and arteriogenic accessory cells. The Journal of Experimental Medicine 210: 2611-2625. DOI: 10.1084/jem.20120690.

Bai G, Matsuba T, Niki T, Hattori T (2020) Stimulation of THP-1 Macrophages with LPS Increased the Production of Osteopontin-Encapsulating Exosome. International Journal of Molecular Sciences 21: 8490. DOI: 10.3390/ijms21228490.

Basile DP, Yoder MC (2014) Circulating and tissue resident endothelial progenitor cells. Journal of Cellular Physiology 229: 10-16. DOI: 10.1002/jcp.24423.

Bouland C, Philippart P, Dequanter D, Corrillon F, Loeb I, Bron D, Lagneaux L, Meuleman N (2021) Cross-Talk Between Mesenchymal Stromal Cells (MSCs) and Endothelial Progenitor Cells (EPCs) in Bone Regeneration. Frontiers in Cell and Developmental Biology 9: 674084. DOI: 10.3389/fcell.2021.674084.

Bouleftour W, Granito RN, Vanden-Bossche A, Sabido O, Roche B, Thomas M, Linossier MT, Aubin JE, Lafage-Proust MH, Vico L, Malaval L (2017) Bone Shaft Revascularization After Marrow Ablation Is Dramatically Accelerated in BSP-/- Mice, Along With Faster Hematopoietic Recolonization. Journal of Cellular Physiology 232: 2528-2537. DOI: 10.1002/jcp.25630.

Chambers SEJ, O'Neill CL, Guduric-Fuchs J, McLoughlin KJ, Liew A, Egan AM, O'Brien T, Stitt AW, Medina RJ (2018) The Vasoreparative Function of Myeloid Angiogenic Cells Is Impaired in Diabetes Through the Induction of IL1β. Stem Cells (Dayton, Ohio) 36: 834-843. DOI: 10.1002/stem.2810.

Chen J, Hendriks M, Chatzis A, Ramasamy SK, Kusumbe AP (2020) Bone Vasculature and Bone Marrow Vascular Niches in Health and Disease. Journal of Bone and Mineral Research: the Official Journal of the American Society for Bone and Mineral Research 35: 2103-2120. DOI: 10.1002/jbmr.4171.

Chintala H, Krupska I, Yan L, Lau L, Grant M, Chaqour B (2015) The matricellular protein CCN1 controls retinal angiogenesis by targeting VEGF, Src homology 2 domain phosphatase-1 and Notch signaling. Development (Cambridge, England) 142: 2364-2374. DOI: 10.1242/dev.121913.

Chopra H, Hung MK, Kwong DL, Zhang CF, Pow EHN (2018) Insights into Endothelial Progenitor Cells: Origin, Classification, Potentials, and Prospects. Stem Cells International 2018: 9847015. DOI: 10.1155/2018/9847015.

Crockett JC, Schütze N, Tosh D, Jatzke S, Duthie A, Jakob F, Rogers MJ (2007) The matricellular protein CYR61 inhibits osteoclastogenesis by a mechanism independent of alphavbeta3 and alphavbeta5. Endocrinology 148: 5761-5768. DOI: 10.1210/en.2007-0473.

Dobin A, Davis CA, Schlesinger F, Drenkow J, Zaleski C, Jha S, Batut P, Chaisson M, Gingeras TR (2013) STAR: ultrafast universal RNA-seq aligner. Bioinformatics (Oxford, England) 29: 15-21. DOI: 10.1093/bioinformatics/bts635.

Everaert BR, Van Laere SJ, Lembrechts R, Hoymans VY, Timmermans JP, Vrints CJ (2019) Identification of Macrophage Genotype and Key Biological Pathways in Circulating Angiogenic Cell Transcriptome. Stem Cells International 2019: 9545261. DOI: 10.1155/2019/9545261.

Fadini GP, Mehta A, Dhindsa DS, Bonora BM, Sreejit G, Nagareddy P, Quyyumi AA (2020a) Circulating stem cells and cardiovascular outcomes: from basic science to the clinic. European Heart Journal 41: 4271-4282. DOI: 10.1093/eurheartj/ehz923.

Fadini GP, Spinetti G, Santopaolo M, Madeddu P (2020b) Impaired Regeneration Contributes to Poor Outcomes in Diabetic Peripheral Artery Disease. Arteriosclerosis, Thrombosis, and Vascular Biology 40: 34-44. DOI: 10.1161/ATVBAHA.119.312863.

Freeberg MA, Fromont LA, D'Altri T, Romero AF, Ciges JI, Jene A, Kerry G, Moldes M, Ariosa R, Bahena S, Barrowdale D, Barbero MC, Fernandez-Orth D, Garcia-Linares C, Garcia-Rios E, Haziza F, Juhasz B, Llobet OM, Milla G, Mohan A, Rueda M, Sankar A, Shaju D, Shimpi A, Singh B, Thomas C, de la Torre S, Uyan U, Vasallo C, Flicek P, et al (2022) The European Genome-phenome Archive in 2021. Nucleic Acids Research 50: D980-D987. DOI: 10.1093/nar/gkab1059.

Girousse A, Mathieu M, Sastourné-Arrey Q, Monferran S, Casteilla L, Sengenès C (2021) Endogenous Mobilization of Mesenchymal Stromal Cells: A Pathway for Interorgan Communication? Frontiers in Cell and Developmental Biology 8: 598520. DOI: 10.3389/fcell.2020.598520.

Grunewald M, Avraham I, Dor Y, Bachar-Lustig E, Itin A, Jung S, Chimenti S, Landsman L, Abramovitch R, Keshet E (2006) VEGF-induced adult neovascularization: recruitment, retention, and role of accessory cells. Cell 124: 175-189. DOI: 10.1016/j.cell.2005.10.036.

Hafen B, Wiesner S, Schlegelmilch K, Keller A, Seefried L, Ebert R, Walles H, Jakob F, Schütze N (2018) Physical contact between mesenchymal stem cells and endothelial precursors induces distinct signatures with relevance to the very early phase of regeneration. Journal of Cellular Biochemistry 119: 9122-9140. DOI: 10.1002/jcb.27175.

Hernandez GE, Iruela-Arispe ML (2020) The many flavors of monocyte/macrophage–endothelial cell interactions. Current Opinion in Hematology 27: 181-189. DOI: 10.1097/MOH.0000000000000573.

Herrmann M, Bara JJ, Sprecher CM, Menzel U, Jalowiec JM, Osinga R, Scherberich A, Alini M, Verrier S (2016) Pericyte plasticity - comparative investigation of the angiogenic and multilineage potential of pericytes from different human tissues. European Cells & Materials 31: 236-249. DOI: 10.22203/ecm.v031a16.

Herrmann M, Binder A, Menzel U, Zeiter S, Alini M, Verrier S (2014) CD34/CD133 enriched bone marrow progenitor cells promote neovascularization of tissue engineered constructs in vivo. Stem Cell Research 13: 465-477. DOI: 10.1016/j.scr.2014.10.005.

Herrmann M, Zeiter S, Eberli U, Hildebrand M, Camenisch K, Menzel U, Alini M, Verrier S, Stadelmann VA (2018) Five Days Granulocyte Colony-Stimulating Factor Treatment Increases Bone Formation and Reduces Gap Size of a Rat Segmental Bone Defect: A Pilot Study. Frontiers in Bioengineering and Biotechnology 6: 5. DOI: 10.3389/fbioe.2018.00005.

Holm E, Gleberzon JS, Liao Y, Sørensen ES, Beier F, Hunter GK, Goldberg HA (2014) Osteopontin mediates mineralization and not osteogenic cell development in vitro. The Biochemical Journal 464: 355-364. DOI: 10.1042/BJ20140702.

Hong H, Tian XY (2020) The Role of Macrophages in Vascular Repair and Regeneration after Ischemic Injury. International Journal of Molecular Sciences 21: 6328. DOI: 10.3390/ijms21176328.

Hoß SG, Schlesinger M, Bendas G (2017) The matricellular ligand Cyr61 contributes to the metastatic spread of tumors by activating integrin VLA-4, independently of thiol redox modulation. International Journal of Clinical Pharmacology and Therapeutics 55: 682-685. DOI: 10.5414/CPXCES15EA03.

Imhof BA, Jemelin S, Ballet R, Vesin C, Schapira M, Karaca M, Emre Y (2016) CCN1/CYR61-mediated meticulous patrolling by Ly6Clow monocytes fuels vascular inflammation. Proceedings of the National Academy of Sciences of the United States of America 113: E4847-E4856. DOI: 10.1073/pnas.1607710113.

Itkin T, Gur-Cohen S, Spencer JA, Schajnovitz A, Ramasamy SK, Kusumbe AP, Ledergor G, Jung Y, Milo I, Poulos MG, Kalinkovich A, Ludin A, Kollet O, Shakhar G, Butler JM, Rafii S, Adams RH, Scadden DT, Lin CP, Lapidot T (2016) Distinct bone marrow blood vessels differentially regulate haematopoiesis. Nature 532: 323-328. DOI: 10.1038/nature17624.

Kapoor A, Gaubert A, Marshall A, Meier IB, Yew B, Ho JK, Blanken AE, Dutt S, Sible IJ, Li Y, Jang JY, Brickman AM, Rodgers K, Nation DA (2021) Increased Levels of Circulating Angiogenic Cells and Signaling Proteins in Older Adults With Cerebral Small Vessel Disease. Frontiers in Aging Neuroscience 13: 711784. DOI: 10.3389/fnagi.2021.711784.

Kawakami Y, Matsumoto T, Mifune Y, Fukui T, Patel KG, Walker GN, Kurosaka M, Kuroda R (2017) Therapeutic Potential of Endothelial Progenitor Cells in the Field of Orthopaedics. Current Stem Cell Research & Therapy 12: 3-13. DOI: 10.2174/1574888x11666160810102945.

Kawamoto A, Katayama M, Handa N, Kinoshita M, Takano H, Horii M, Sadamoto K, Yokoyama A, Yamanaka T, Onodera R, Kuroda A, Baba R, Kaneko Y, Tsukie T, Kurimoto Y, Okada Y, Kihara Y, Morioka S, Fukushima M, Asahara T (2009) Intramuscular transplantation of G-CSF-mobilized CD34(+) cells in patients with critical limb ischemia: a phase I/IIa, multicenter, single-blinded, dose-escalation clinical trial. Stem Cells (Dayton, Ohio) 27: 2857-2864. DOI: 10.1002/stem.207.

Kireeva ML, Lam SC, Lau LF (1998) Adhesion of human umbilical vein endothelial cells to the immediate-early gene product Cyr61 is mediated through integrin alphavbeta3. The Journal of Biological Chemistry 273: 3090-3096. DOI: 10.1074/jbc.273.5.3090.

Kohara Y, Kitazawa R, Haraguchi R, Imai Y, Kitazawa S (2022) Macrophages are requisite for angiogenesis of type H vessels during bone regeneration in mice. Bone 154: 116200. DOI: 10.1016/j.bone.2021.116200.

Kusumbe AP, Ramasamy SK, Adams RH (2014) Coupling of angiogenesis and osteogenesis by a specific vessel subtype in bone. Nature 507: 323-328. DOI: 10.1038/nature13145.

Landers-Ramos RQ, Sapp RM, Shill DD, Hagberg JM, Prior SJ (2019) Exercise and Cardiovascular Progenitor Cells. Comprehensive Physiology 9: 767-797. DOI: 10.1002/cphy.c180030.

Lee GS, Salazar HF, Joseph G, Lok ZSY, Caroti CM, Weiss D, Taylor WR, Lyle AN (2019) Osteopontin isoforms differentially promote arteriogenesis in response to ischemia via macrophage accumulation and survival. Laboratory Investigation; a Journal of Technical Methods and Pathology 99: 331-345. DOI: 10.1038/s41374-018-0094-8.

Leu SJ, Chen N, Chen CC, Todorovic V, Bai T, Juric V, Liu Y, Yan G, Lam SCT, Lau LF (2004) Targeted mutagenesis of the angiogenic protein CCN1 (CYR61). Selective inactivation of integrin alpha6beta1-heparan sulfate proteoglycan coreceptor-mediated cellular functions. The Journal of Biological Chemistry 279: 44177-44187. DOI: 10.1074/jbc.M407850200.

Leu SJ, Liu Y, Chen N, Chen CC, Lam SCT, Lau LF (2003) Identification of a novel integrin alpha 6 beta 1 binding site in the angiogenic inducer CCN1 (CYR61). The Journal of Biological Chemistry 278: 33801-33808. DOI: 10.1074/jbc.M305862200.

Liao Y, Smyth GK, Shi W (2014) featureCounts: an efficient general purpose program for assigning sequence reads to genomic features. Bioinformatics (Oxford, England) 30: 923-930. DOI: 10.1093/bioinformatics/btt656.

Lienau J, Schell H, Epari DR, Schütze N, Jakob F, Duda GN, Bail HJ (2006) CYR61 (CCN1) protein expression during fracture healing in an ovine tibial model

and its relation to the mechanical fixation stability. Journal of Orthopaedic Research: Official Publication of the Orthopaedic Research Society 24: 254-262. DOI: 10.1002/jor.20035.

Löbel M, Bauer S, Meisel C, Eisenreich A, Kudernatsch R, Tank J, Rauch U, Kühl U, Schultheiss HP, Volk HD, Poller W, Scheibenbogen C (2012) CCN1: a novel inflammation-regulated biphasic immune cell migration modulator. Cellular and Molecular Life Sciences: CMLS 69: 3101-3113. DOI: 10.1007/s00018-012-0981-x.

Lok ZSY, Lyle AN (2019) Osteopontin in Vascular Disease. Arteriosclerosis, Thrombosis, and Vascular Biology 39: 613-622. DOI: 10.1161/ATVBAHA.118.311577.

Love MI, Huber W, Anders S (2014) Moderated estimation of fold change and dispersion for RNA-seq data with DESeq2. Genome Biology 15: 550. DOI: 10.1186/s13059-014-0550-8.

Luque-Martin R, Mander PK, Leenen PJM, Winther MPJ (2021) Classic and new mediators for in vitro modelling of human macrophages. Journal of Leukocyte Biology 109: 549-560. DOI: 10.1002/JLB.1RU0620-018R.

Maniatis K, Siasos G, Oikonomou E, Vavuranakis M, Zaromytidou M, Mourouzis K, Paraskevopoulos T, Charalambous G, Papavassiliou AG, Tousoulis D (2020) Osteoprotegerin and Osteopontin Serum Levels are Associated with Vascular Function and Inflammation in Coronary Artery Disease Patients. Current Vascular Pharmacology 18: 523-530. DOI: 10.2174/1570161117666191022095246.

McNeill B, Vulesevic B, Ostojic A, Ruel M, Suuronen EJ (2015) Collagen matrix-induced expression of integrin $\alpha V\beta 3$ in circulating angiogenic cells can be targeted by matricellular protein CCN1 to enhance their function. FASEB Journal: Official Publication of the Federation of American Societies for Experimental Biology 29: 1198-1207. DOI: 10.1096/fj.14-261586.

Mead LE, Prater D, Yoder MC, Ingram DA (2008) Isolation and characterization of endothelial progenitor cells from human blood. Current Protocols in Stem Cell Biology Chapter 2: Unit 2C.1. DOI: 10.1002/9780470151808.sc02c01s6.

Medina RJ, Barber CL, Sabatier F, Dignat-George F, Melero-Martin JM, Khosrotehrani K, Ohneda O, Randi AM, Chan JKY, Yamaguchi T, Van Hinsbergh VWM, Yoder MC, Stitt AW (2017) Endothelial Progenitors: A Consensus Statement on Nomenclature. Stem Cells Translational Medicine 6: 1316-1320. DOI: 10.1002/sctm.16-0360.

Medina RJ, O'Neill CL, Sweeney M, Guduric-Fuchs J, Gardiner TA, Simpson DA, Stitt AW (2010) Molecular analysis of endothelial progenitor cell (EPC) subtypes reveals two distinct cell populations with different identities. BMC Medical Genomics 3: 18. DOI: 10.1186/1755-8794-3-18.

Mo FE, Muntean AG, Chen CC, Stolz DB, Watkins SC, Lau LF (2002) CYR61 (CCN1) is essential for placental development and vascular integrity. Molecular and Cellular Biology 22: 8709-8720. DOI: 10.1128/MCB.22.24.8709-8720.2002.

Mohandas R, Diao Y, Chamarthi G, Krishnan S, Agrawal N, Wen X, Dass B, Shukla AM, Gopal S, Koç M, Segal MS (2021) Circulating endothelial cells as predictor of long-term mortality and adverse cardiovascular outcomes in hemodialysis patients. Seminars in Dialysis 34: 163-169. DOI: 10.1111/sdi.12943.

Müller-Deubert S, Ege C, Krug M, Meißner-Weigl J, Rudert M, Bischof O, Jakob F, Ebert R (2020) Phosphodiesterase 10A Is a Mediator of Osteogenic Differentiation and Mechanotransduction in Bone Marrow-Derived Mesenchymal Stromal Cells. Stem Cells International 2020: 7865484. DOI: 10.1155/2020/7865484.

Murphy-Ullrich JE, Sage EH (2014) Revisiting the matricellular concept. Matrix Biology: Journal of the International Society for Matrix Biology 37: 1-14. DOI: 10.1016/j.matbio.2014.07.005.

Orecchioni M, Ghosheh Y, Pramod AB, Ley K (2019) Macrophage Polarization: Different Gene Signatures in M1(LPS+) vs. Classically and M2(LPS-) vs. Alternatively Activated Macrophages. Frontiers in Immunology 10: 1084. DOI: 10.3389/fimmu.2019.01084.

Orozco SL, Canny SP, Hamerman JA (2021) Signals governing monocyte differentiation during inflammation. Current Opinion in Immunology 73: 16-24. DOI: 10.1016/j.coi.2021.07.007.

Perbal B (2018) The concept of the CCN protein family revisited: a centralized coordination network. Journal of Cell Communication and Signaling 12: 3-12. DOI: 10.1007/s12079-018-0455-5.

Pfaffl MW (2001) A new mathematical model for relative quantification in real-time RT-PCR. Nucleic Acids Research 29: e45. DOI: 10.1093/nar/29.9.e45.

Pireaux V, Delporte C, Rousseau A, Desmet JM, Van Antwerpen P, Raes M, Zouaoui Boudjeltia K (2021) M2 Monocyte Polarization in Dialyzed Patients Is Associated with Increased Levels of M-CSF and Myeloperoxidase-Associated Oxidative Stress: Preliminary Results. Biomedicines 9: 84. DOI: 10.3390/biomedicines9010084.

Plein A, Fantin A, Denti L, Pollard JW, Ruhrberg C (2018) Erythro-myeloid progenitors contribute endothelial cells to blood vessels. Nature 562: 223-228. DOI: 10.1038/s41586-018-0552-x.

Ponzetti M, Rucci N (2019) Updates on Osteoimmunology: What's New on the Cross-Talk Between Bone and Immune System. Frontiers in Endocrinology 10: 236. DOI: 10.3389/fendo.2019.00236.

Rafii S, Butler JM, Ding BS (2016) Angiocrine functions of organ-specific endothelial cells. Nature 529: 316-325. DOI: 10.1038/nature17040.

Ramasamy SK, Kusumbe AP, Schiller M, Zeuschner D, Bixel MG, Milia C, Gamrekelashvili J, Limbourg A,

Medvinsky A, Santoro MM, Limbourg FP, Adams RH (2016) Blood flow controls bone vascular function and osteogenesis. Nature Communications 7: 13601. DOI: 10.1038/ncomms13601.

Ramasamy SK, Kusumbe AP, Wang L, Adams RH (2014) Endothelial Notch activity promotes angiogenesis and osteogenesis in bone. Nature 507: 376-380. DOI: 10.1038/nature13146.

Rehman J, Li J, Orschell CM, March KL (2003) Peripheral blood "endothelial progenitor cells" are derived from monocyte/macrophages and secrete angiogenic growth factors. Circulation 107: 1164-1169. DOI: 10.1161/01.cir.0000058702.69484.a0.

Sabbah N, Tamari T, Elimelech R, Doppelt O, Rudich U, Zigdon-Giladi H (2019) Predicting Angiogenesis by Endothelial Progenitor Cells Relying on In-Vitro Function Assays and VEGFR-2 Expression Levels. Biomolecules 9: 717. DOI: 10.3390/biom9110717.

Schlecht A, Zhang P, Wolf J, Thien A, Rosmus DD, Boneva S, Schlunck G, Lange C, Wieghofer P (2021) Secreted Phosphoprotein 1 Expression in Retinal Mononuclear Phagocytes Links Murine to Human Choroidal Neovascularization. Frontiers in Cell and Developmental Biology 8: 618598. DOI: 10.3389/fcell.2020.618598.

Schlundt C, El Khassawna T, Serra A, Dienelt A, Wendler S, Schell H, van Rooijen N, Radbruch A, Lucius R, Hartmann S, Duda GN, Schmidt-Bleek K (2018) Macrophages in bone fracture healing: Their essential role in endochondral ossification. Bone 106: 78-89. DOI: 10.1016/j.bone.2015.10.019.

Schmid M, Kropfl JM, Spengler CM (2021) Changes in Circulating Stem and Progenitor Cell Numbers Following Acute Exercise in Healthy Human Subjects: a Systematic Review and Meta-analysis. Stem Cell Reviews and Reports 17:1091-1120. DOI:10.1007/s12015-020-10105-7.

Schmitz P, Gerber U, Schütze N, Jüngel E, Blaheta R, Naggi A, Torri G, Bendas G (2013) Cyr61 is a target for heparin in reducing MV3 melanoma cell adhesion and migration via the integrin VLA-4. Thrombosis and Haemostasis 110: 1046-1054. DOI: 10.1160/TH13-02-0158.

Schütze N, Kunzi-Rapp K, Wagemanns R, Nöth U, Jatzke S, Jakob F (2005) Expression, purification, and functional testing of recombinant CYR61/CCN1. Protein Expression and Purification 42: 219-225. DOI: 10.1016/j.pep.2005.03.031.

Schütze N, Schenk R, Fiedler J, Mattes T, Jakob F, Brenner RE (2007) CYR61/CCN1 and WISP3/CCN6 are chemoattractive ligands for human multipotent mesenchymal stroma cells. BMC Cell Biology 8: 45. DOI: 10.1186/1471-2121-8-45.

Seefried L, Müller-Deubert S, Krug M, Youssef A, Schütze N, Ignatius A, Jakob F, Ebert R (2017) Dissection of mechanoresponse elements in promoter sites of the mechanoresponsive CYR61 gene. Experimental Cell Research 354: 103-111. DOI: 10.1016/j.yexcr.2017.03.031.

Shi Y, Kramer G, Schröder A, Kirkpatrick CJ, Seekamp A, Schmidt H, Fuchs S (2014) Early endothelial progenitor cells as a source of myeloid cells to improve the pre-vascularisation of bone constructs. European Cells & Materials 27: 64-64–79; discussion 79–80. DOI: 10.22203/ecm.v027a06.

Sivaraj KK, Adams RH (2016) Blood vessel formation and function in bone. Development (Cambridge, England) 143: 2706-2715. DOI: 10.1242/dev.136861.

Soltero EG, Solovey AN, Hebbel RP, Palzer EF, Ryder JR, Shaibi GQ, Olson M, Fox CK, Rudser KD, Dengel DR, Evanoff NG, Kelly AS (2021) Relationship of Circulating Endothelial Cells With Obesity and Cardiometabolic Risk Factors in Children and Adolescents. Journal of the American Heart Association 10: e018092. DOI: 10.1161/JAHA.120.018092.

Spiller KL, Nassiri S, Witherel CE, Anfang RR, Ng J, Nakazawa KR, Yu T, Vunjak-Novakovic G (2015) Sequential delivery of immunomodulatory cytokines to facilitate the M1-to-M2 transition of macrophages and enhance vascularization of bone scaffolds. Biomaterials 37: 194-207. DOI: 10.1016/j.biomaterials.2014.10.017.

Stucker S, Chen J, Watt FE, Kusumbe AP (2020) Bone Angiogenesis and Vascular Niche Remodeling in Stress, Aging, and Diseases. Frontiers in Cell and Developmental Biology 8: 602269. DOI: 10.3389/fcell.2020.602269.

Su JL, Chiou J, Tang CH, Zhao M, Tsai CH, Chen PS, Chang YW, Chien MH, Peng CY, Hsiao M, Kuo ML, Yen ML (2010) CYR61 regulates BMP-2-dependent osteoblast differentiation through the {alpha}v{beta}3 integrin/integrin-linked kinase/ERK pathway. The Journal of Biological Chemistry 285: 31325-31336. DOI: 10.1074/jbc.M109.087122.

Tardelli M, Zeyda K, Moreno-Viedma V, Wanko B, Grün NG, Staffler G, Zeyda M, Stulnig TM (2016) Osteopontin is a key player for local adipose tissue macrophage proliferation in obesity. Molecular Metabolism 5: 1131-1137. DOI: 10.1016/j.molmet.2016.09.003.

Varol C, Mildner A, Jung S (2015) Macrophages: development and tissue specialization. Annual Review of Immunology 33: 643-675. DOI: 10.1146/annurev-immunol-032414-112220.

Vianello E, Kalousová M, Dozio E, Tacchini L, Zima T, Corsi Romanelli MM (2020) Osteopontin: The Molecular Bridge between Fat and Cardiac-Renal Disorders. International Journal of Molecular Sciences 21: 5568. DOI: 10.3390/ijms21155568.

Wing TT, Erikson DW, Burghardt RC, Bazer FW, Bayless KJ, Johnson GA (2020) OPN binds alpha V integrin to promote endothelial progenitor cell incorporation into vasculature. Reproduction (Cambridge, England) 159: 465-478. DOI: 10.1530/REP-19-0358.

Wolf AA, Yáñez A, Barman PK, Goodridge HS (2019) The Ontogeny of Monocyte Subsets. Frontiers in Immunology 10: 1642. DOI: 10.3389/fimmu.2019.01642.

Yahara Y, Ma X, Gracia L, Alman BA (2021) Monocyte/Macrophage Lineage Cells From Fetal Erythromyeloid Progenitors Orchestrate Bone Remodeling and Repair. Frontiers in Cell and Developmental Biology 9: 622035. DOI: 10.3389/fcell.2021.622035.

Yoder MC (2018) Endothelial stem and progenitor cells (stem cells): (2017 Grover Conference Series). Pulmonary Circulation 8: 2045893217743950. DOI: 10.1177/2045893217743950.

Yu G, Wang LG, Han Y, He QY (2012) clusterProfiler: an R package for comparing biological themes among gene clusters. Omics: a Journal of Integrative Biology 16: 284-287. DOI: 10.1089/omi.2011.0118.

Yuan Q, Jiang Y, Zhao X, Sato T, Densmore M, Schüler C, Erben RG, McKee MD, Lanske B (2014) Increased osteopontin contributes to inhibition of bone mineralization in FGF23-deficient mice. Journal of Bone and Mineral Research: the Official Journal of the American Society for Bone and Mineral Research 29: 693-704. DOI: 10.1002/jbmr.2079.

Zhao G, Huang BL, Rigueur D, Wang W, Bhoot C, Charles KR, Baek J, Mohan S, Jiang J, Lyons KM (2018) CYR61/CCN1 Regulates Sclerostin Levels and Bone Maintenance. Journal of Bone and Mineral Research: the Official Journal of the American Society for Bone and Mineral Research 33: 1076-1089. DOI: 10.1002/jbmr.3394.

Editor's note: The Scientific Editor responsible for this paper was Juerg Gasser.